DIPARTIMENTO SCIENZE DELLA VITA

DOTTORATO DI RICERCA IN SCIENZE DELLA VITA

LIFE SCIENCES

CICLO XXXVI

COORDINATRICE Prof.ssa Simona Maccherini

Unveiling new targets to overcome the extended Chronic Lymphocytic Leukemia cells survival

SETTORE SCIENTIFICO-DISCIPLINARE: BIO/11

TUTOR: Prof. Laura Patrussi

DOTTORANDA: Dr. Gioia Boncompagni

Gioia Boncompagni
18.02.2024 14:49:38
GMT+01:00

A.A. 2022-2023

INDEX

ABSTRACT **3**

INTRODUCTION **5**

1.1 Chronic Lymphocytic Leukemia (CLL) **5**

1.1.1 Epidemiology and aetiology 5

1.1.2 Diagnosis 5

1.2 Mechanisms underlying the extended CLL cell survival **6**

Part I **9**

Glycerophosphoinositol promotes apoptosis of Chronic Lymphocytic Leukemia cells by enhancing Bax expression and activation **9**

INTRODUCTION **10**

1.1 Glycerophosphoinositols (GPIs) **10**

1.2 The tyrosine phosphatase SHP-1 ..... **12**

AIMS **14**

MATERIALS AND METHODS **15**

2.1 Purification and culture of human primary B cells **15**

2.2 Reagents **17**

2.3 Cell Treatments, Antibodies and Immunoblots **17**

2.4 Intracellular Staining, Apoptosis, TMRM Assays and Flow Cytometry **17**

2.5 GroPIns-Bio Pull-Down Assay **18**

2.6 RNA Isolation, Reverse Transcription and qRT-PCR **19**

2.7 Statistical Analyses **19**

RESULTS **20**

3.1 GroPIns has a pro-apoptotic activity on CLL cells which depends on SHP-1 ..... **20**

3.2 GroPIns enhances the expression of Bax in CLL cells in a SHP-1-dependent manner **21**

3.3 GroPIns interacts with and activates Bax in CLL cells **22**

3.4 GroPIns enhances the pro-apoptotic effects of Venetoclax on CLL cells **25**

DISCUSSION **27**

Part II **30**

Leukemic cell-secreted interleukin-9 suppresses cytotoxic T cell-mediated killing in Chronic Lymphocytic Leukemia **30**

INTRODUCTION **31**

1.1 Mechanisms of immune evasion in the TME **31**

1.1.1 The PD-1/PD-L1 immune checkpoint axis 31
1.1.2 CTL-mediated killing of tumor cells 32
1.2 The molecular adaptor p66Shc and its deficiency in CLL cells 33
AIMS 36
MATERIAL AND METHODS 37
2.1 CLL patients, healthy donors, mice and cell lines 37
2.2 Conditioned supernatants and multiplex assays 38
2.3 Purification, activation and conditioning of $CD8^+$ cells 38
2.4 Immune synapse formation, immunofluorescence and analysis 40
2.5 Degranulation and Cytotoxicity assays 40
2.6 CLL cell Ibrutinib treatments and ELISA assays 41
2.7 In vivo Ibrutinib treatment of CLL patients 41
2.8 RNA purification, gene expression profiling, qRT-PCR 41
2.9 Flow cytometry and viability assays 42
2.10 Statistical analyses 42
RESULTS 43
3.1 Soluble factors released by CLL cells enhance PD-1 expression in CTLs and suppress their ability to assemble functional ISs 43
3.2 The p66Shc expression defect in CLL cells contributes to their soluble PD-1-elevating and IS-disrupting activity 47
3.3 p66Shc deficiency in leukemic cells from Eμ-TCL1 mice enhances their soluble PD1-elevating activity on $CD8^+$ cells 49
3.4 p66Shc deficiency impinges on the cytokine landscape of CLL cells 50
3.5 IL-9 secreted by leukemic cells from CLL patients promotes PD-1 expression in CTLs 54
3.6 IL-9 secreted by leukemic cells from CLL patients impairs IS formation in CTLs 56
3.7 In vivo IL-9 blockade in Eμ-TCL1/$p66^{-/-}$ mice normalizes PD-1 expression in $CD8^+$ cells 58
8. Ex vivo and in vivo inhibition of BTK enhances IL-9 expression in leukemic cells from CLL patients 58
DISCUSSION 60
BIBLIOGRAPHY 63

ABSTRACT

Chronic Lymphocytic Leukemia (CLL) is characterized by the accumulation of mature B cells in peripheral blood and lymphoid organs. The extended survival of leukemic cells is due to a combination of intrinsic alterations in the apoptotic machinery and microenvironmental factors, which both mediate evasion of immune surveillance. Among intrinsic alteration, the profound imbalance in the expression of pro- and anti-apoptotic members of the Bcl-2 family stands out. Impaired activity of the phosphatase SHP-1 in CLL cells has been related to the deficient expression of the pro-apoptotic Bcl-2 family member Bax. Since the membrane phospholipid metabolite glycerophosphoinositol (GroPIns) binds and activates SHP-1, here we asked whether GroPIns can restore Bax expression in CLL cells by reactivating SHP-1. To test this hypothesis, we cultured CLL cells in the presence of GroPIns, alone or in combination with Venetoclax, a Bcl-2 inhibitor commonly used for CLL treatment. We found that GroPIns alone increases Bax expression and apoptosis in CLL cells in a SHP-1 dependent manner. Moreover, GroPIns potentiates the pro-apoptotic activity of Venetoclax. Interestingly, among GroPIns interactors, we found Bax itself, which becomes activated when CLL cells are treated with GroPIns. These data provide evidence that GroPIns exploits two different pathways converging on Bax to promote leukemic cell apoptosis.

Surface receptor/ligand inhibitory axes have recently reached attention as promoters of CLL cell survival in the tumor microenvironment (TME) by suppressing the killing activities of cytotoxic T cells (CTLs) and their ability to form the immune synapse (IS), a specialized platform which polarizes both membrane and soluble signaling mediators at the interface between T cell and antigen-presenting cell. Since leukemic cells release soluble factors which profoundly shape the TME toward a pro-survival and protective niche, here we asked whether they also contribute to suppress CTL anti-tumoral functions. We found that healthy CTLs cultured in media conditioned by leukemic cells from CLL patients or Eμ-TCL1 mice upregulate the exhaustion marker PD-1 and become unable to form functional ISs and kill target cells. These defects were more pronounced when media were conditioned by leukemic cells lacking the pro-apoptotic adaptor p66Shc, whose deficiency has been implicated in CLL aggressiveness. Multiplex ELISA assays and quantitative RT-PCR showed that interleukin (IL)-9 and IL-10 were overexpressed in leukemic cells from CLL patients, where they inversely correlated with residual p66Shc. Using neutralizing antibodies or the recombinant cytokines we show that IL-9, but not IL-10, mediates both the enhancement in PD-1 expression and the suppression of effector functions in healthy CTLs. These data demonstrate that IL-9 secreted by leukemic cells negatively modulates the anti-tumor immune abilities of CTLs.

Altogether, our results highlight new intrinsic and extrinsic mechanisms underlying the defective apoptosis of CLL cells, and pave the way to new studies aimed at exploiting these molecular pathways as therapeutical targets in CLL.

INTRODUCTION

1.1 Chronic Lymphocytic Leukemia (CLL)

1.1.1 Epidemiology and aetiology

Chronic Lymphocytic Leukemia (CLL) is a lymphoproliferative disorder characterized by the accumulation of mature $CD5^+/CD19^+$ B cells in peripheral blood, bone marrow, lymph nodes, and spleen.[1] CLL is the most common leukemia among adults in the Western world, with an incidence of approximately 4 cases per 100,000 people per year.[2] Typically diagnosed in individuals with a median age of 67-72 years, CLL is often regarded as a disease affecting the elderly. Nevertheless, in the last decades, a growing number of younger individuals, nearly 15% of patients, have been diagnosed around the age of 55.[1,2]

The aetiology of this pathology remains unknown, since exposure to common carcinogens does not appear to be linked to disease onset. Ongoing studies are exploring potential connections between the onset of CLL and inflammation and/or autoimmune conditions.[3]

Remarkably, hereditary genetic susceptibility plays a significant role in CLL. It is well-documented that 8-10% of cases have a family history of the disease.[4] Relatives of CLL patients have a heightened risk of developing CLL and other lymphoproliferative disorders when compared to the general population, although the genetic basis of this susceptibility remains elusive.[1]

1.1.2 Diagnosis

Most CLL patients are asymptomatic at the time of diagnosis, and the disease is detected due to an increased lymphocyte count during blood evaluations performed for unrelated reasons.[2] However, CLL patients can present a wide range of clinical symptoms. These may include weight loss, fever, fatigue, and an increased frequency of infections which may be associated with hypogammaglobulinemia or autoimmune cytopenia that in turn may induce immunodeficiency and increased risk of infection-related mortality.[1,2,5] Some patients do not experience disease progression and can live without treatment need. Conversely, patients with aggressive disease require immediate treatment.[2]

The 2018 iwCLL (International Workshop on Chronic Lymphocytic Leukemia) guidelines give recommendations on diagnostic criteria for CLL. In most cases CLL diagnosis is established by blood count, blood smear, and immunophenotyping:

1. the diagnosis requires detection of ≥ 5,000 B lymphocytes per µl of peripheral blood, sustained for at least 3 months. Lymphocytes in the blood smear are characteristically small (7-10 µm diameter) and mature, with poor cytoplasm and dense nuclei lacking discernible nucleoli with partially aggregated chromatin. Gumprecht shadows, which are degenerated cells broken during slide preparation, are also present in peripheral blood smears (**Fig. 1**);[2]

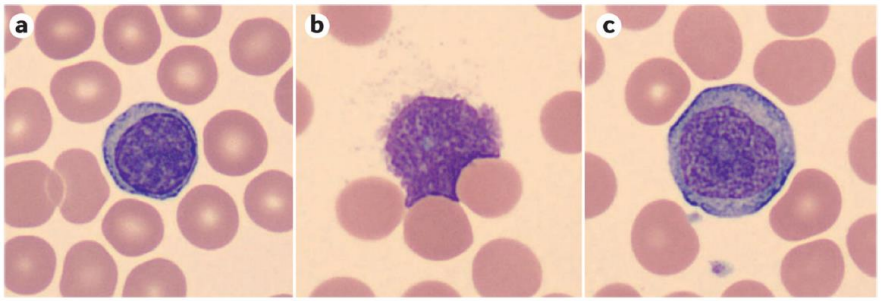

Figure 1. Peripheral blood smear of CLL patients. Wright-Giemsa-stained blood smears showing the typical CLL B lymphocyte (**a**), Gumprecht shadow or smudge cell (**b**) and a prolymphocyte with a prominent nucleolus (**c**). Magnification ×500 (adapted from Kipps *et al.*[1]).

2. CLL immunophenotype is characterized by three elements:

   a) the expression of low levels of surface immunoglobulins (Igs) with restricted light chains (κ or λ);

   b) the co-expression of the T cell-specific antigen CD5 and the B cell surface antigens CD19 and CD20;

   c) low levels of the BCR-associated signaling molecule Igβ (also known as CD79b) and surface Igs, that in CLL appear to be mainly IgM; it is not unusual to find IgM and IgD co-expression.[2]

1.2 Mechanisms underlying the extended CLL cell survival

CLL patients are characterized by a high percentage of B cells that progressively accumulate in bone marrow, lymphoid organs, and peripheral blood, where they are mainly arrested in the G0/G1 phase of the cell cycle. Only few of them proliferate in "pseudo-germinal centres" located in both bone marrow and lymph nodes.[6]

Of key importance for the pathogenesis of this disease, CLL cells display extended survival,[7] which can be attributed to a combination of intrinsic alterations in the apoptotic program[8] and extrinsic factors provided by the tumor microenvironment (TME), which help them evading the anti-tumor immune responses.[9] Among intrinsic factors, CLL cells exhibit an altered balance of members of

the B-cell lymphoma-2 (Bcl-2) family of apoptosis-regulating proteins,[8] which play a key role in regulating mitochondrial apoptosis.[10] Bcl-2 itself belongs to the group of anti-apoptotic and pro-survival members, which also includes MCL-1, BCL2L1, and Bcl-w. The group of pro-apoptotic Bcl-2 family members includes Bax and Bak which, upon activation, homo-oligomerize and lead to permeabilization of the mitochondrial membrane, thereby promoting cytochrome *c* release, caspase activation, and apoptosis.[8,10]

Many researchers have reported altered expression of the Bcl-2 family members in CLL, with enhanced levels of the anti-apoptotic Bcl-2 and MCL-1 alongside downregulation of the pro-apoptotic proteins Bax and Bak.[8,11] The decreased Bcl-2/Bax ratio has been associated with both increased sensitivity of CLL cells to cytotoxic drugs in *vitro* and improved response to chemotherapy in *vivo*. Indeed, resistance to apoptosis of leukemic cells is associated with disease progression and an inadequate response to treatment.[1]

It was previously shown that 13q deletion [del(13q)], the most common cytogenetic abnormality in CLL patients, leads to deletion of the microRNAs miR-15 and miR-16, which act as negative regulators of Bcl-2 expression.[12] However, the fact that an altered balance of Bcl-2 family members is observed in the majority of cases suggests that intrinsic mechanisms other than miR-15 and miR-16 deletion are operational in this malignancy which alter their expression.

Not only intrinsic factors, but also external, microenvironmental-derived factors contribute to extend CLL cell survival. Indeed, when CLL cells are maintained in *vitro* alone, they recover their ability to undergo apoptosis, suggesting that extrinsic factors present in the TME are required for their survival.[13,14] This has been elegantly demonstrated by Willimott and colleagues, who reported that CLL cells cultured in the presence of recombinant CD40 ligand (CD40L), a surface glycoprotein expressed by several immune cells including $CD4^+$ and $CD8^+$ T lymphocytes, upregulate Bcl-2 and show extended survival.[15] In line with these findings, several studies have shown that CLL cell survival significantly increases when they are cultured in the presence of stromal and immune cells of the TME[16] which provide extrinsic factors, including surface ligands, cytokines and chemokines, which favour their survival.

The TME consists of various types of accessory cells, including stromal cells, nurse-like cells (NLCs) and endothelial cells. The TME also includes cells of both innate and adaptive immunity, such as dendritic cells (DCs), Natural Killer (NK) cells, $CD4^+$ and $CD8^+$ T lymphocytes and regulatory T cells (Tregs). Leukemic cells themselves shape the TME by secreting chemokines such as CCL3, CCL4, and CCL22, cytokines such as IL-10, and other soluble mediators that recruit immune cells in this niche,[6,17] thereby contributing to establish an inflammatory, immunosuppressive and pro-survival milieu.[18]

Several studies have documented alterations in the T cell repertoire in CLL patients, which show increased total numbers of $CD4^+$ and $CD8^+$ T lymphocytes, with a shift in their ratio towards $CD8^+$ lymphocytes, likely as a result of an attempted adaptive immune response targeted against CLL cells.[19,20] Interestingly, as a consequence of chronic antigenic stimulation, T lymphocytes lose their effector functions and become "exhausted" and unable to eliminate cancer cells.[21] The "exhausted" T cell phenotype is characterized by increased expression of inhibitory receptors such as Cytotoxic T-Lymphocyte Antigen-4 (CTLA-4), Lymphocyte Activation Gene-3 (LAG-3) and Programmed Cell Death-1 (PD-1),[18] coupled with an inability to produce adequate levels of immune-activating cytokines during stimulation.[21] CLL cells contribute to the "exhausted" phenotype of T cells thanks to the enhanced expression of inhibitory surface ligands which interact with the inhibitory receptors expressed by T lymphocytes. This mechanism has been found to suppress the effector functions of cytotoxic T lymphocytes (CTLs), which differentiate from naïve $CD8^+$ T cells[22] to eliminate both infected and tumor cells by building the immunological synapse (IS), a highly specialized structure that allows for target cell killing.[23] Importantly, a profound impairment in IS formation favours CLL cell escape from CTL-mediated killing.[22]

The formation of a distinctive TME, coupled with the interaction and influence of factors derived from it, enables CLL cells to evolve alongside the microenvironment. How intrinsic factors, such as the tilted balance between anti- and pro-apoptotic intrinsic factors, and extrinsic factors coming from the TME, crosstalk to enhance growth and prolong survival of leukemic cells remains still elusive and represents a significant focus of investigation in CLL.

Part I

Glycerophosphoinositol promotes apoptosis of Chronic Lymphocytic Leukemia cells by enhancing Bax expression and activation

Part I

INTRODUCTION

1.1 Glycerophosphoinositols (GPIs)

Glycerophosphoinositols (GPIs) are ubiquitous water-soluble bioactive compounds which can be detected both in the cytoplasm and in the extracellular space. Their intracellular concentrations are cell-type dependent and their production vary upon oncogenic transformation, cellular differentiation and hormonal stimulation.[24]

GPIs exist as both unphosphorylated (glycerophosphoinositol (GroPIns)) and phosphorylated (glycerophosphoinositol 4-phosphate (GroPIns4P) and glycerophosphoinositol 4,5-biphosphate (GroPIns 4,5 P2)) metabolites. GroPIns and GroPIns4P are generated starting from the membrane phospholipids phosphatidylinositol (PtdIns) and PtdIns4-phosphate (PtdIns4P), respectively.[24] Their production requires the enzyme phospholipase A_2IVα (PLA2IVα), that has both intrinsic phospholipase and lysolipase activities.[25] Indeed, GroPIns formation requires two sequential deacylation steps, both carried out by PLA2IVα. The first reaction involves hydrolysis of membrane PtdIns to free arachidonic acid and lysophosphatidylinositol (LysoPtdIns), while the second deacylation reaction releases free GroPIns and fatty acid from LysoPtdIns (**Fig. 2**).

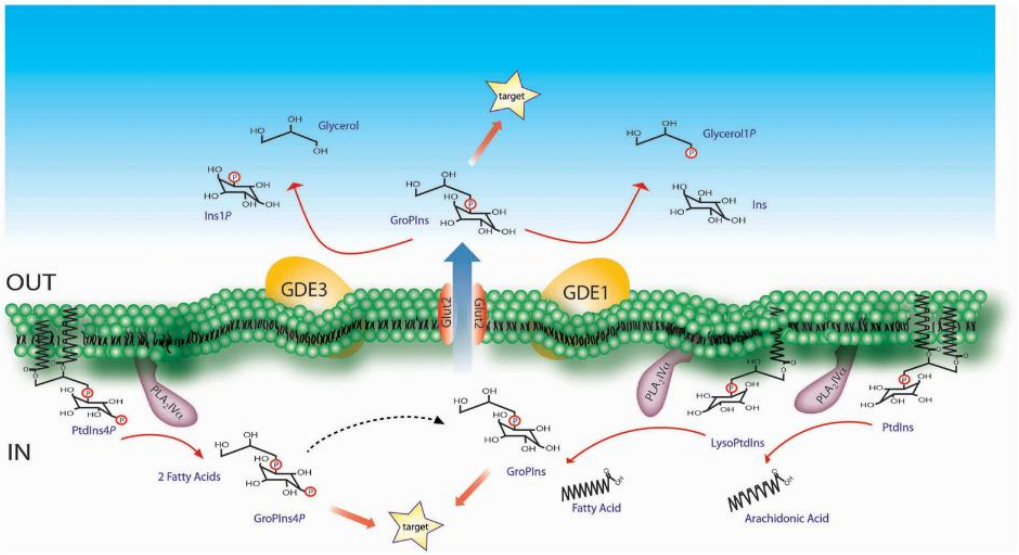

Figure 2. Schematic representation of the GroPIns metabolism GroPIns is produced from membrane PtdIns via two sequential deacylation reactions catalysed by PLA2IVα. The first reaction produces LysoPtdIns and free arachidonic acid, while the second reaction releases free fatty acid and GroPIns. GroPIns can be active on intracellular targets or can be released in the extracellular space through the Glut2 transporter. In the extracellular space GroPIns can either behave as a paracrine molecule or be catabolised by GDEs. (adapted from Patrussi *et al.*[26]).

GroPIns4P formation, also schematized in **figure 2**, occurs starting from membrane PtdIns4P following the same diacylation cascade operated by PLA2IVα.[26]

Once produced in the cytoplasm, both GroPIns and GroPIns4P can act on intracellular targets. GroPIns is also transported to the extracellular space through the Glut2 transporter, where it can act as a paracrine factor on nearby target cells.[24] In the extracellular space, GroPIns is degraded thanks to the membrane-bound glycerophosphodiesterases GDE1 and GDE3, which catalyse the hydrolysis of extracellular GroPIns to glycerolphosphate and glycerol (**Fig. 2**).[24]

The amounts of GPIs, especially GroPIns and GroPIns4P, have been monitored in a wide variety of cells.[27,28] While GroPIns ranges from low micromolar to almost millimolar concentrations,[27] the relative levels of GroPIns4P have been found to be approximately 10-fold lower.[27,29] Interestingly, the amounts of GroPIns change during differentiation of both myeloid and lymphoid cells.[30–32] Studies conducted on cell lines representative of the immature and mature stages of B and T lymphocytes showed a significant increase in GroPIns levels in mature cells.[31] These changes in the intracellular concentrations of GroPIns indicate a potential role for this metabolite in regulating both myeloid and lymphoid cell differentiation.

Pro-inflammatory stimuli increase intracellular levels of GPIs, in macrophages, suggesting that these metabolites are implicated in modulating immune responses. Indeed, macrophages release GroPIns and GroPIns4P in the extracellular space, where they promote recruitment of T lymphocytes.[28]

The release of these metabolites has been recently shown to be involved in T lymphocyte signaling. When exogenously added, GroPIns4P activates Lck, a member of the Src family of tyrosine kinases which is responsible for initiation of the T cell receptor (TCR) signaling cascade, which in turn activates the Rho-family dependent pathway, which promotes actin polymerization.[33] Interestingly, treatment of T lymphocytes with GroPIns4P also promotes chemotaxis toward the homeostatic chemokine CXCL12, demonstrating the potent immunomodulatory effect of this compound.[33]

In innate immune cells, GPIs negatively regulate the expression of pro-inflammatory mediators. When exogenously added, GroPIns acts as an anti-inflammatory factor by blocking the Toll-like Receptor 4 (TLR4)-dependent signaling cascade triggered by lipopolysaccharide (LPS) in human blood monocytes, thereby leading to decreased NF-κB-dependent transcription of pro-inflammatory genes.[34]

Thus, GPIs exploit different functions according to the specific target/receptor. Exogenous addition of GPIs could therefore contribute to not only modulate pro-inflammatory responses, but also counteract the invasive potential of tumor cells and build efficient anti-tumor immune responses in malignancies characterised by low levels of these metabolites.

1.2 The tyrosine phosphatase SHP-1

In lymphocytes, the tight balance between phosphatases and kinases strictly regulates several cellular processes, including cell growth, migration, invasion, differentiation and survival.[35] Indeed, deviations in the phosphorylation/dephosphorylation balance have been found to promote the abnormal intracellular accumulation of phosphorylated proteins, which in turn cause signaling pathway alterations.[35]

The tyrosine phosphatase SHP-1 (Src homology region 2 (SH2) domain-containing phosphatase-1) is one of the fundamental regulators of inflammatory and immune responses. It contains two SH2 domains at the N-terminus, a central catalytic phosphatase domain and a C-terminal tail containing several tyrosine phosphorylation sites.[36] SHP-1 is expressed in both epithelial and hematopoietic cells, where it negatively regulates several pathways mediated by cytokine, chemokine and growth factor receptors.[37]

By dephosphorylating key signaling mediators, SHP-1 has been found to act as tumor suppressor in both haematological and solid cancers. Indeed, its down-regulation or absence promotes tumor progression.[38] These findings, together with the fact that SHP-1 promotes tumor cell apoptosis by suppressing the oncogenic JAK/STAT3 pathway, which controls the expression of a series of genes encoding anti-apoptotic (Bcl-2, BCL2L1) and pro-apoptotic proteins (Cyclin D1),[38] strongly suggest that targeting SHP-1 may represent a suitable anti-cancer strategy.

Several chemotherapeutic drugs, like Surafenib,[39] and natural compounds targeting SHP-1, such as dietary xanthone α-mangostin (α-MGT)[40] and Phloretin[41], counteract tumor cell proliferation by inducing SHP-1-mediated dephosphorylation of STAT3. Importantly, Gan and colleagues demonstrated that the in *vitro* treatment of Acute Promyelocytic Leukemia cells with epigallocatechin-3 gallate, a polyphenol with biochemical antioxidant properties, promotes tumor cell apoptosis by activating SHP-1, which in turn upregulates the expression of the pro-apoptotic protein Bax.[42]

CLL is characterized by failure in the apoptotic process, which not only depends on the alteration in the expression of pro- and anti-apoptotic members of the Bcl-2 family,[8] but also by inhibition of SHP-1 activity. Indeed, despite leukemic cells exhibit SHP-1 expression levels comparable to those observed in healthy B cells, its activity is inhibited due to constitutive phosphorylation of the Serine 591 (pS591) residue in the C-terminal tail.[43] The existence of a pool of inactive SHP-1 in CLL cells is crucial for escaping apoptosis program, as demonstrated by the fact that SHP-1 inhibition through either pharmacological or genetic approaches results in reduced activation of the caspase cascade and impaired apotosis.[44] Additionally, SHP-1 activity can be promoted by Nintedanib, a small molecule known to act as angiokinase inhibitor.[43] In breast cancer cells, Nintedanib has been found

to activate SHP-1 by blocking S591 phosphorylation, leading to the dephosphorylation of pro-apoptotic players such as caspases and serine/threonine phosphatase 2A (PP2A), thereby normalizing apoptosis.[43] These results suggest that reactivation of SHP-1 in CLL cells may restore their ability to undergo apoptosis, and make of this phosphatase an interesting pharmacological target for the treatment of CLL.

Thanks to mass spectrometry analyses performed on melanoma cells, Varone and colleagues recently reported that GroPIns directly interacts with SHP-1.[37] This interaction promotes SHP-1 localization at invadopodia,[45] where it dephosphorylates cortactin.[46] This condition leads to a reduction in the metastatic capacity of melanoma cells both in *vitro* and in *vivo*,[46] suggesting that the interaction between GroPIns and SHP-1 has an anti-tumor potential. The fact that SHP-1 promotes the expression of Bax in Acute Promyelocytic Leukemia cells further confirms that it is an interesting target of future studies.

Part I

AIMS

GroPIns is a biomolecule which pleiotropically affects key cellular functions.[26] It has been recently demonstrated that GroPIns interacts with the phosphatase SHP-1,[37] a known promoter of the expression of the pro-apoptotic protein Bax in Acute Promyelocytic Leukemia cells.[42] Since in CLL cells, the phosphatase activity of SHP-1 is impaired,[1,8] here we asked whether GroPIns may promote apoptosis of CLL cells by activating SHP-1 and in turn enhancing Bax expression.

Part I

MATERIALS AND METHODS

2.1 Purification and culture of human primary B cells

The collection of peripheral blood samples from anonymous healthy donors was approved by the local ethics committee (Siena University Hospital and Padova University Hospital) and performed after receiving signed informed consent according to institutional guidelines.

Peripheral blood samples were collected from 40 treatment naïve CLL patients. Diagnosis of CLL was made according to international workshop on CLL (iwCLL) 2018 criteria.[2] The immunophenotypic analysis of lymphocytes obtained from peripheral blood of CLL patients was performed by flow cytometry. All patients were positive for CD19, CD5, CD23 and CD200. Mutational *IGHV* status was assessed as reported.[47] The main clinical features of CLL patients used in this study are listed in **Table 1.**

B cells from 24 buffy coats were used as healthy population controls. B cells were purified by negative selection using RosetteSep B-cell enrichment Cocktail (StemCell Technologies, Vancouver, Canada) followed by density gradient centrifugation on Lympholite (Cedarlane Laboratories, The Netherlands), as reported in manufacturer's instructions.

Cells were maintained in RPMI (Roswell Park Memorial Institute)-1640 (Merck, #R8758) supplemented with 7.5% Bovine Calf Serum (BCS) (HyClone, #SH30072.03) and penicillin 50 IU/ml.

CLL Patient	Mutational *IGHV* status	Karyotype	WBC (n/µl)	Ly % (n/µl)
# 1	mutated	wild-type	7.910	41.2
# 2	mutated	wild-type	17.590	65.2
# 3	mutated	13q	24.730	79.6
# 4	mutated	13q	12.900	66.2
# 5	mutated	13q	52.810	nd
# 6	mutated	wild-type	16.380	72.5
# 7	mutated	13q	10.770	67.8
# 8	mutated	11q	9.210	92.0
# 9	unmutated	13q	86.940	92.0
# 10	unmutated	13q	10.580	62.6
# 11	mutated	12+	83.750	69.2
# 12	unmutated	13q	47.830	97.0
# 13	mutated	11q	27.120	69.4
# 14	unmutated	17p	39.420	91.3
# 15	mutated	13q	32.960	93.0
# 16	unmutated	11q	69.100	81.6
# 17	unmutated	17p	19.900	70.3
# 18	unmutated	wild-type	113.700	96.6
# 19	unmutated	12+	35.190	73.6
# 20	unmutated	13q	58.120	88.2
# 21	unmutated	17p	74.660	90.6
# 22	unmutated	13q	79.450	95.6
# 23	unmutated	13q	39.070	95.5
# 24	mutated	13q	36.850	91.7
# 25	mutated	13q	22.450	77.7
# 26	unmutated	13q	206.800	98.5
# 27	unmutated	12+	65.700	86.2
# 28	mutated	13q	30.000	83.7
# 29	mutated	13q	66.400	88.7
# 30	unmutated	11q	121.900	96.0
# 31	mutated	13q	198.000	97.0
# 32	unmutated	11q	106.100	94.5
# 33	unmutated	12+	66.900	93.3
# 34	mutated	13q	88.230	90.9
# 35	unmutated	11q	124.900	95.9
# 36	mutated	wild-type	26.680	83.9
# 37	mutated	13q	15430	81.4
# 38	mutated	wild-type	43600	82.6
# 39	unmutated	17p	23600	67.8
# 40	mutated	wild-type	69740	94.0

Table 1. Clinical parameters of CLL patients used in this study. IGHV: Immunoglobulin heavy variable chain; WBC: white blood cell count; Ly: lymphocytes.

2.2 Reagents

GroPIns was kindly provided by Euticals S.P.A. (Lodi, Italy). GroPIns-Bio was obtained from Echelon Biosciences (Salt Lake City, UT, USA). NSC-87887 (#565851) was from Merck and Venetoclax was from Selleck Chemicals (#S8048). His-tagged Bax-α lacking 21 amino acids at the C-terminus (His-BaxDTM) cloned in the pTrcHis vector (Invitrogen Srl) was a kind gift of Ingram Iaccarino. This construct was expressed in *E. coli* BL21(DE3)/ pLysS cells and purified as described [48].

2.3 Cell Treatments, Antibodies and Immunoblots

Treatments with 100 μM GroPIns, 3.5 nM Venetoclax or combination treatments were carried out at 37°C in RPMI 7.5% BCS for the indicated times. Control samples were treated with DMSO (Merck Millipore, #102952). When required, cells were pretreated at 37°C for 20 min with 50 mM NSC-87887. Cells (5×10^6 cells/sample) were lysed in 1% (v/v) Triton X-100 in 20 mM Tris-HCl pH 8, 150 mM NaCl, in the presence of a cocktail of protease inhibitors (Calbiochem, #539134) and 0.2 mg/ml Na orthovanadate (Merck, #S6508), resolved by SDS-PAGE and transferred to nitrocellulose (GE Healthcare, #9004-70-0). Immunoblots were carried out using mouse anti-Bax (BD Biosciences, #610982), anti-penta-His (Life Technologies, #P21315) and anti-actin (Millipore, #MAB1501) primary antibodies. Secondary peroxidase-labeled anti-mouse antibodies were from Jackson Immuno-Research (#115-035-146). Labeled antibodies were detected using ECL kit (SuperSignal® West Pico Chemiluminescent Substrate, Thermo Scientific) and scanned immunoblots were quantified using the ImageJ software.

2.4 Intracellular Staining, Apoptosis, TMRM Assays and Flow Cytometry

Cells (2×10^5 cells/sample) were treated for 20 min in complete medium at 37°C as above, washed with PBS and fixed in 100 μl of fixation buffer (eBiosciences, #420801) for 15 minutes at Room Temperature (RT). Cells were then washed with PBS added with 1% BSA (AppliChem PanReac, #A6588) and incubated with 10 μl permeabilization buffer (eBiosciences, #421008) containing either mouse anti-Bax (B-9) (Santa Cruz Biotechnology Inc., #sc-7480) or rabbit anti-phospho-SHP-1 Tyrosine 564 (Cell Signaling, #D11G5) antibodies at RT for 1 h, washed twice in PBS 1% BSA and then incubated with 10 μl permeabilization buffer containing Alexa Fluor anti-mouse-488 (Thermo Fisher Scientific, #A11001) or anti-rabbit-488 (Thermo Fisher Scientific, #A11008) secondary antibodies for 45 min. After washing with PBS 1% BSA, cell pellets were resuspended in 200 μl PBS 1% BSA and subjected to flow cytometric analysis. Early apoptotic cells were

quantified by flow cytometric analysis of 1×10^6 cells stained with FITC-labeled Annexin V (e-Bioscience, #88-8005-74) and Propidium iodide (PI, 20 μg/mL, Biotium, #40017). Mitochondrial membrane potential was measured using the fluorescent probe tetramethylrhodamine methyl ester (TMRM, Molecular Probes Europe BV). Cells (10^6 cells/sample) were suspended in 200 μl RPMI-1640 w/o phenol Red (Invitrogen srl) added with 25 mM Hepes pH 7.4 and 200 nM TMRM and incubated for 20 min at 37°C. Cells were then added with 500 ng/ml of the calcium ionophore A23187 (Sigma-Aldrich #C7522), incubated for 10 min at 37°C and subjected to flow cytometric analysis. Flow cytometry was carried out using a Guava Millipore cytometer as described [49]. Data were analysed using Flowjo (Tree Star, Inc.).

2.5 GroPIns-Bio Pull-Down Assay

GroPIns-Bio pull-down assays were previously described [37]. Briefly, Raw 264.7 cells were centrifuged, washed with PBS and re-suspended in lysis buffer supplemented with a protease inhibitor cocktail (Complete Mini EDTA-free, Roche). The cell lysate was kept on a rotating wheel for 30 min at 4°C, centrifuged and the supernatant recovered, brought to a 0.2% (w/v) final concentration of Triton X-100, and dialyzed at 4°C. The cell extract was then precleared on 1 mg of uncoupled streptavidin-conjugated paramagnetic beads (Invitrogen Srl) on a rotating wheel, recovered and incubated with 1 mg of streptavidin-conjugated beads previously incubated with 2.5 nmoles of GroPIns-Bio (from Echelon Biosciences (Salt Lake City, UT, USA)) or biotin in binding buffer (50 mM Tris-HCl, pH 7.6, 50 mM KCl, 10 mM EDTA) supplemented with the protease inhibitor cocktail. Following incubation, the unbound materials were separated, and the beads were washed with binding buffer.

GroPIns-bound proteins were specifically eluted with 5 mM GroPIns. The elution was performed for 30 min at 4°C on a rotating wheel, eluted proteins were recovered, resuspended in SDS sample buffer and analysed by SDS-PAGE. Protein bands were analysed by liquid chromatography coupled to tandem mass spectrometry (LC/MS-MS). For GroPIns-Bio pull-down assays with purified Bax, 100 ng of purified His-Bax were incubated for 2 h at 4°C with 0.5 mg of streptavidin-conjugated paramagnetic beads in the presence of 2.5 nmoles of biotin (Sigma-Aldrich, #B4501) or GroPIns-Bio in binding buffer plus protease inhibitors (Complete Mini EDTA-free, Roche). Following incubation, the unbound material was removed, and beads were washed with binding buffer. The beads with bound protein were boiled in 100 μl of SDS sample buffer.

2.6 RNA Isolation, Reverse Transcription and qRT-PCR

For all the experiments RNA was extracted from samples by using the RNeasy Plus Mini Kit (Qiagen) according to the manufacturer's instructions, and RNA purity and concentration were measured using QIAxpert (Qiagen). Single strand cDNAs were generated using the iScriptTM cDNA Synthesis Kit 28 (Bio-Rad), and qRT-PCR was performed using the SsoFastTM EvaGreenR supermix kit (Bio-Rad) and specific pairs of primers listed in **Table 2**. Samples were run in triplicate on 96-well optical PCR plates (Sarstedt AG, Nümbrecht, Germany). Values are expressed as ΔΔCT relative to housekeeping gene HPRT1 expression.

Gene	Forward 5'-3'	Reverse 5'-3'
Bax	GAGAGGTCTTTTTCCGACTGG	CCTTGAGCACCAGTTTGCTG
Bcl-2	GGAGGCTGGGATGCCTTT	CCAGATAGGCACCCAGGGT
MCL-1	GCTGGGAGTTGGTCGGGGA	TCGTAAGGTCTCCAGCGCCT
B2CL1	ATGAACTCTTCCGGGATGG	TGGATCCAAGGCTCTAGGTG
HPRT1	AGATGGTCAAGGTCGCAAG	GTATTCATTATAGTCAAGGGCATATC

Table 2. List of primers used in this study.

2.7 Statistical Analyses

One-way ANOVA with post-hoc Tukey was used for experiments where multiple groups were compared. Mann Whitney rank-sum tests were performed to determine the significance of the differences between two groups. Statistical analyses were performed using GraphPad Software (La Jolla, CA). *P* values <0.05 were considered significant.

Part I

RESULTS

3.1 GroPIns has a pro-apoptotic activity on CLL cells which depends on SHP-1

GroPIns is a naturally occurring phosphoinositide metabolite whose intracellular concentrations depend on the cell type. Its production changes in response to oncogenic transformation, cell differentiation and hormonal stimulation.[24] In melanoma cells, GroPIns interacts with the tyrosine phosphatase SHP-1,[38] which is known to promote apoptosis by enhancing Bax expression.[42]

The activity of SHP-1 has been shown to be impaired in CLL cells.[43] Thus, to investigate whether GroPIns reactivates SHP-1, we first examined whether it promotes apoptosis of leukemic cells through a SHP-1-dependent mechanism. B cells purified from peripheral blood of CLL patients and healthy donors (HD) were cultured for 24 h at 37°C in the presence of 100 μM GroPIns, and the percentage of early apoptotic Annexin V^+/PI^- cells was quantified by flow cytometry. Our results showed that GroPIns significantly enhanced apoptosis of CLL cells (**Fig. 3A, 3B**). Apoptosis of healthy B cells was also enhanced, although at significantly lower levels compared to CLL cells (**Fig. 3A, 3B**). The SHP-1-specific inhibitor NSC-87887 partly reversed the pro-apoptotic effect of GroPIns (**Fig. 3B**), demonstrating that it at least in part relies on the tyrosine phosphatase activity of SHP-1.

In melanoma cells, GroPIns binds SHP-1 and induces the dephosphorylation of the actin-binding and cytoskeletal protein cortactin, thereby reducing their invasive capacity.[37] To understand whether GroPIns interacts with and activates SHP-1 in CLL cells, B cells purified from peripheral blood of CLL patients and healthy donors were cultured for 30 min at 37°C in the presence of GroPIns and the phosphorylated form of SHP-1 was quantified by flow cytometry using an antibody recognizing the phosphorylated tyrosine 564.[50] Our results showed that basal SHP-1 phosphorylation levels were significantly lower in CLL cells compared to healthy B cells (**Fig. 3C, 3D**). Following GroPIns treatment, SHP-1 phosphorylation increased in healthy B cells, and the increase was significantly more pronounced in CLL cells (**Fig. 3C, 3D**). These data suggest that GroPIns promotes CLL cell apoptosis by activating SHP-1.

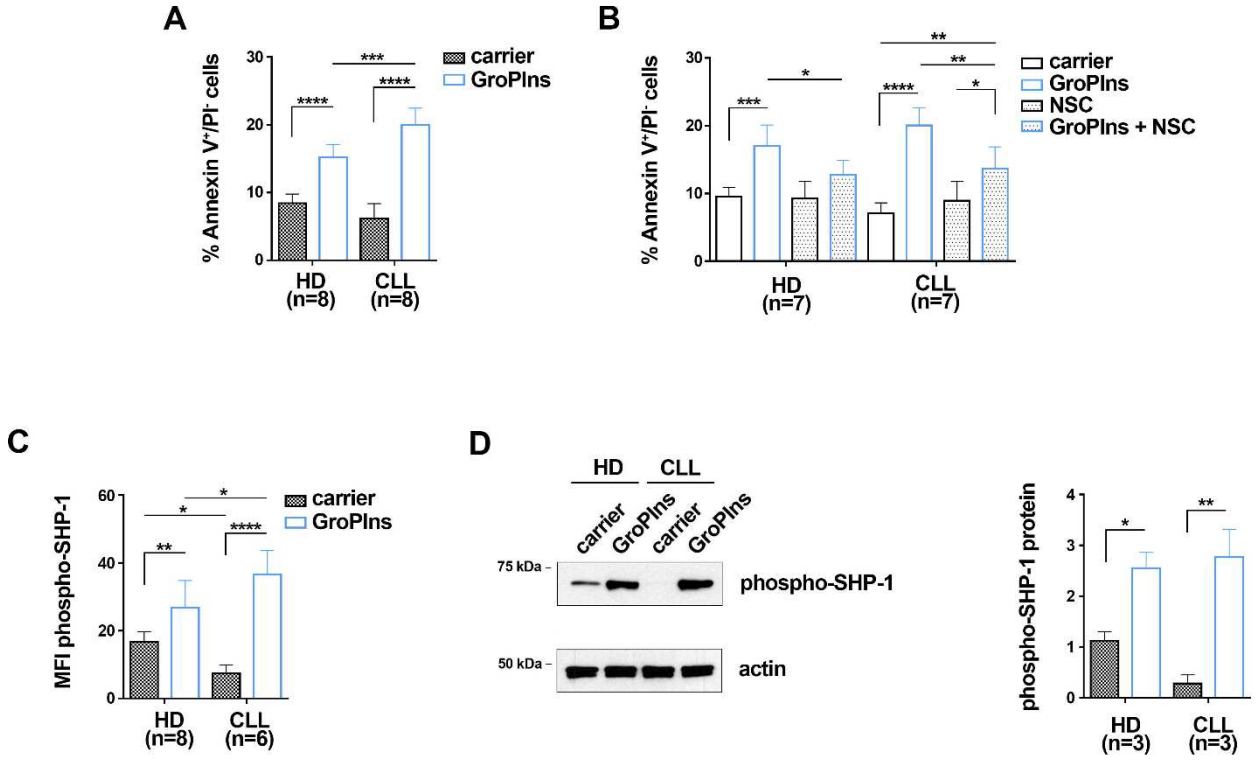

Figure 3 GroPIns promotes CLL cell apoptosis in a SHP-1-dependent manner. (A) Flow cytometric analysis of the percentages of Annexin V^+/PI^- cells in B lymphocytes from HD (n=8) and CLL (n=8) after treatment with either carrier or 100 µM GroPIns for 24 h at 37°C. **(B)** Flow cytometric analysis of the percentages of Annexin V^+/PI^- cells in B cells from HD (n=7) and CLL (n=7). Samples were treated for 24 h at 37°C with either carrier or 100 µM GroPIns in the presence or absence of 50 µM NSC-87887 (NSC). **(C)** Flow cytometric analysis of phospho-SHP-1 in B cells from HD (n=8) and CLL (n=6), treated with either carrier or 100 µM GroPIns for 30 min at 37°C. Data are expressed as MFI phospho-SHP-1 in live cells. **(D)** Immunoblot of phospho-SHP-1 protein expression in B lymphocytes from HD (n=3) and CLL (n=3), after treatment as in (C). The stripped filters were reprobed with anti-actin antibodies. Molecular weights (kDa) are indicated on the left of the panel. The quantification of three independent experiments is shown on the right. Mean ± SD. ANOVA two-way test, Multiple Comparison. $p \leq 0.0001$, ****; $p \leq 0.001$, ***; $p \leq 0.01$, **; $p \leq 0.05$, *.

3.2 GroPIns enhances the expression of Bax in CLL cells in a SHP-1-dependent manner

In CLL cells, altered apoptosis depends in part on the decreased expression of the pro-apoptotic protein Bax.[8] Since the activation of SHP-1 enhances Bax expression and increases apoptosis in Acute Promyelocytic Leukemia cells, we aimed to understand whether GroPIns promotes apoptosis in CLL cells by increasing Bax expression in a SHP-1-dependent manner. B cells were purified from peripheral blood of CLL patients and healthy donors and cultured for 24 h at 37°C in the presence of GroPIns. Bax expression was assessed by both immunoblot and qRT-PCR. As expected, untreated CLL cells expressed lower levels of Bax compared to healthy B cells (**Fig. 4A - 4C**).

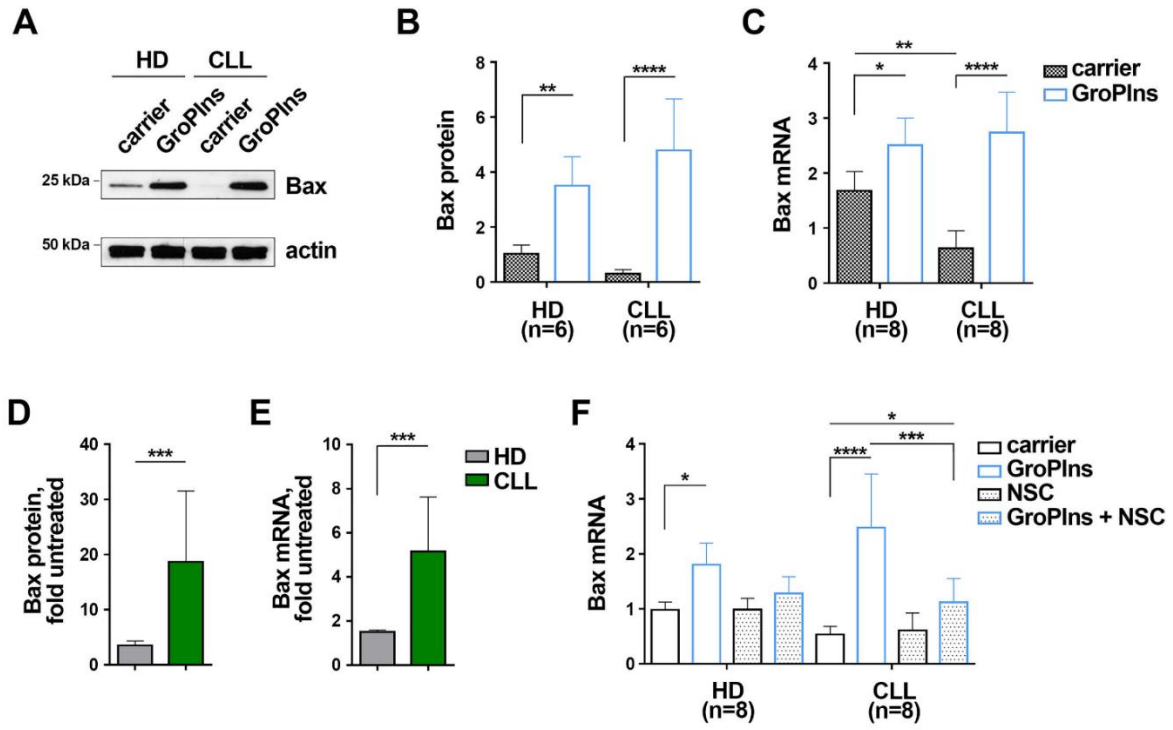

Figure 4. GroPIns promotes Bax expression in CLL cells. (A, B) Immunoblot analysis of Bax protein expression in B lymphocytes from HD (n=6) and CLL (n=6), after treatment with either carrier or 100 µM GroPIns for 24 h at 37°C. The stripped filters were reprobed with anti-actin antibodies. Molecular weights (kDa) are indicated on the left of the panel. **(B, C)** qRT-PCR analysis of Bax mRNA in B cells from HD (n=8) and CLL (n=8), treated as in (A) and (B). **(D, E)** Fold protein (D) and mRNA (E) expression levels of Bax in samples from HD and CLL. Data were calculated as fold Bax protein quantification of treated vs untreated samples shown in (B, C). **(F)** qRT-PCR analysis of Bax mRNA in B cells from HD (n=8) and CLL (n=7), treated for 24 h at 37°C with either carrier or 100 µM GroPIns in the presence or absence of 50 µM NSC-87887 (NSC). (D, E): Mann Whitney Rank Sum Test. $p \leq 0.0001$, ****; $p \leq 0.001$, ***; $p \leq 0.01$, **; $p \leq 0.05$, *.

GroPIns enhanced Bax expression in both healthy and leukemic cells (**Fig. 4A - 4C**). Of note, when Bax expression was calculated as a ratio between treated and untreated samples, it was significantly higher in CLL cells compared to healthy B cells (**Fig. 4D, 4E**). To test whether the Bax-elevating activity of GroPIns depends on the phosphatase activity of SHP-1, both CLL and healthy B cells were treated for 24 h at 37°C with NSC-87887 and Bax expression was assessed by qRT-PCR. Our results show that NCS-87887 abolished the GroPIns-dependent Bax increase, demonstrating that GroPIns promotes CLL cells apoptosis by enhancing Bax expression in a SHP-1-dependent manner (**Fig 4F**).

3.3 GroPIns interacts with and activates Bax in CLL cells

SHP-1 has been previously identified as a direct cellular target of GroPIns through a pull-down assay coupled with liquid chromatography-tandem mass-spectrometry analysis.[46] Among direct

interactors of GroPIns (listed in **Table 3**), Varone and colleagues also found Bax. We validated the direct binding of GroPIns with Bax through in vitro pull-down assays. B cells were purified from peripheral blood of CLL patients and healthy donors and treated with 100 µM GroPIns for 24 h at 37°C. The immunoblot in **figure 5A** shows that GroPIns-Bio-bound beads, but not control Biotin-bound beads, specifically pooled-down recombinant Bax, suggesting a direct binding of GroPIns to Bax.

Following pro-apoptotic stimulation, Bax undergoes a conformational change that exposes its N-terminus, shifting it to an active mediator of cell apoptosis.[51] We assessed whether GroPIns promotes Bax activation. B cells from CLL patients and healthy donors were treated with either carrier or 100 µM GroPIns for 20 min at 37°C and Bax activation was quantified by flow cytometry, using an anti-Bax antibody designed to specifically recognize the N-terminus of Bax. Our results show significantly lower basal levels of active Bax in CLL cells compared to the healthy ones (**Fig. 5B, 5C**). When exogenously added, GroPIns enhanced Bax activation in both healthy and CLL cells. Interestingly, when the amount of active Bax was normalized to the protein levels of Bax of untreated cells shown in **figure 4B**, we observed a huge increase of Bax activation in CLL cells, but not in healthy B cells (**Fig. 5C**). Moreover, the increase in Bax activation calculated as the ratio between the MFI of active Bax in treated and untreated samples shown in **figure 5D**, was significantly higher in CLL cells compared to healthy ones (**Fig. 5D**). Consequently, GroPIns selectively induced the activation of Bax in leukemic cells. To assess whether GroPIns restores apoptosis in CLL cells, we quantified mitochondrial depolarization using the fluorescent probe TMRM. Both CLL and healthy B cells were treated for 4 h with either GroPIns or the calcium ionophore A23187, a potent inducer of apoptosis. GroPIns significantly enhanced mitochondrial depolarization in CLL cells, but not in the healthy counterparts (**Fig. 5E**). It is noteworthy that the SHP-1 inhibitor NSC-87887 did not further enhance Bax activation in CLL cells treated with GroPIns (**Fig. 5F**), suggesting that GroPIns-mediated Bax activation does not depend on SHP-1. Collectively, these findings support the existence of two distinct pathways, one dependent on, and the other independent of SHP-1, that both converge on Bax, and suggest that GroPIns takes advantage of both pathways to promote apoptosis of CLL cells.

Swiss-Prote Code	Protein Name
O55143	Sarcoplasmic/endoplasmic reticulum calcium ATPase 2
Q8CGC7	Bifunctional glutamate/proline–tRNA ligase
Q9JKR6	Hypoxia up-regulated protein 1
Q8BMJ2	Leucine–tRNA ligase, cytoplasmic
P70248	Unconventional myosin-If
Q64514	Tripeptidyl-peptidase 2
Q8K4Z5	Splicing factor 3A subunit 1
Q9EQK5	Major vault protein
Q60597	2-oxoglutarate dehydrogenase, mitochondrial
Q8BIJ6	Isoleucine–tRNA ligase, mitochondrial
Q9DBT5	AMP deaminase 2
Q61881	DNA replication licensing factor MCM7
Q9D0R2	Threonine–tRNA ligase 1, cytoplasmic
Q9JIK5	Nucleolar RNA helicase 2
Q9Z110	Delta-1-pyrroline-5-carboxylate synthetase
P26043	Radixin
Q80UM7	Mannosyl-oligosaccharide glucosidase
Q8BML9	Glutamine–tRNA ligase
Q8CHW4	Translation initiation factor eIF-2B subunit epsilon
Q8BNW9	Kelch repeat and BTB domain-containing protein 11
Q99MN1	Lysine–tRNA ligase
Q9WUA2	Phenylalanine–tRNA ligase beta subunit
P29351	Tyrosine-protein phosphatase non-receptor type 6 (Shp1)
P80316	T-complex protein 1 subunit epsilon
Q8BMF4	Dihydrolipoamide acetyltransferase PDH-E2
Q8BP47	Asparagine–tRNA ligase, cytoplasmic
Q91WQ3	Tyrosine–tRNA ligase, cytoplasmic
Q9DBG6	Dolichyl-diphosphooligosaccharide–protein glycosyltransferase subunit 2
Q61024	Asparagine synthetase
P09405	Nucleolin
Q61656	Probable ATP-dependent RNA helicase DDX5
P30416	Peptidyl-prolyl cis-trans isomerase FKBP4
Q99K87	Serine hydroxymethyltransferase, mitochondrial
P47738	Aldehyde dehydrogenase, mitochondrial
Q9Z0N1	Eukaryotic translation initiation factor 2 subunit 3
P80314	T-complex protein 1 subunit beta
P26443	Glutamate dehydrogenase 1, mitochondrial
Q9CZ44	NSFL1 cofactor p47
O88986	2-amino-3-ketobutyrate coenzyme A ligase, mitochondrial
Q922R8	Protein disulfide-isomerase A6
Q9DC69	NADH dehydrogenase 1 alpha subcomplex subunit 9
Q9DB05	Alpha-soluble NSF attachment protein
Q99LC5	Electron transfer flavoprotein subunit alpha, mitochondria
Q64674	Spermidine synthase
Q9CR57	60S ribosomal protein L14
P35278	Ras-related protein Rab-5C
P84099	60S ribosomal protein L19
P20108	Thioredoxin-dependent peroxide reductase, mitochondrial
P61087	Ubiquitin-conjugating enzyme E2 K
P08030	Adenine phosphoribosyltransferase
P62821	Ras-related protein Rab-1°
Q9CZM2	60S ribosomal protein L15
Q9Z1B5	Mitotic spindle assembly checkpoint protein MAD2A
Q62159	Rho-related GTP-binding protein RhoC
P51410	60S ribosomal protein L9
Q9JM14	5'(3')-deoxyribonucleotidase, cytosolic type
P61028	Ras-related protein Rab-8B
P29391	Ferritin light chain 1
P53994	Ras-related protein Rab-2A
P53994	Ras-related protein Rab-2A
P70296	Phosphatidylethanolamine-binding protein 1
P19253	60S ribosomal protein L13a
P08030	Adenine phosphoribosyltransferase
P00375	Dihydrofolate reductase
O09167	60S ribosomal protein L21
Q07813	Apoptosis regulator BAX
Q9EQU5	Protein SET
P62301	40S ribosomal protein S13
P17742	Peptidyl-prolyl cis-trans isomerase A
P62281	40S ribosomal protein S11

Table 3. List of proteins identified from proteomic analysis.

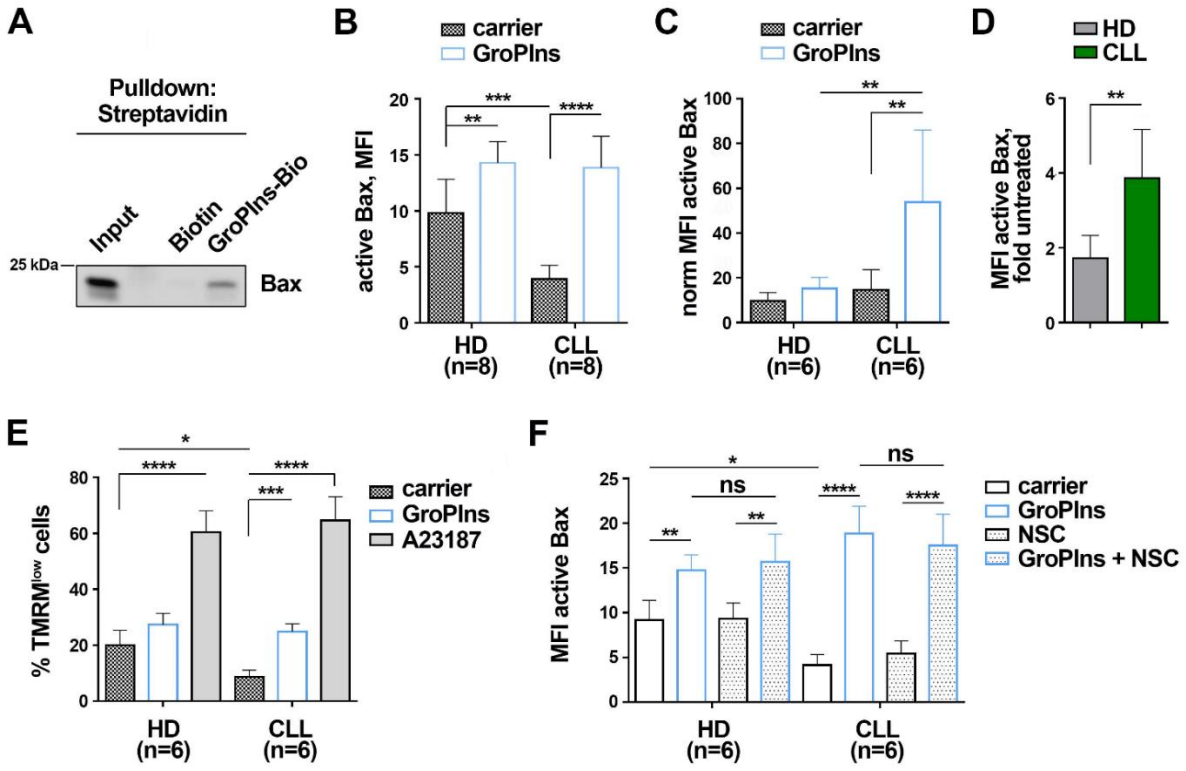

Figure 5. GroPIns interacts with and activates Bax. (A) Representative pull-down of streptavidin-conjugated beads using Biotin or biotinylated GroPIns (GroPIns-Bio) with His-Bax. Eluted proteins were analysed by immunoblot using anti-His antibodies. Molecular weights (kDa) are indicated on the left of the panel. **(B)** Flow cytometric analysis of active Bax in B lymphocytes from HD (n=8) and CLL (n=8). Samples were treated for 20 min at 37°C with either carrier or 100 µM GroPIns. **(C)** The MFI of active Bax shown in panel (B) was normalized to Bax protein levels of untreated cells shown in **figure 4B** (n=6). **(D)** Fold MFI active Bax in samples from HD and CLL shown in panel (C). Data were calculated as fold MFI of active Bax of treated vs. untreated samples. **(E)** Flow cytometric analysis of the percentage of $TMRM^{low}$ cells in B cells from HD (n=6) and CLL (n=6). Samples were treated for 4 h at 37°C with either carrier or 100 µM GroPIns or 500 ng/ml A23187. Stainings were performed in duplicate. **(F)** Flow cytometric analysis of active Bax in B cells from HD (n=6) and CLL (n=6). Samples were treated for 20 min at 37°C with either carrier or 100 µM GroPIns in the presence or in the absence of 50 µM NSC-87887. Mean ± SD. (B, C, E, F): ANOVA two-way test, Multiple Comparison. (D): Mann Whitney Rank Sum Test. $p \leq 0.0001$, ****; $p \leq 0.001$, ***; $p \leq 0.01$, **; $p \leq 0.05$, *; ns, not significant.

3.4 GroPIns enhances the pro-apoptotic effects of Venetoclax on CLL cells

Venetoclax is a drug approved for the treatment of refractory CLL patients that specifically inhibits the anti-apoptotic protein Bcl-2.[52] Ramani and colleagues demonstrated that Venetoclax induces rapid and pronounced activation and mitochondrial translocation of Bax in acute myeloid leukemia cell lines.[53] These data led us to hypothesize that GroPIns enhances the pro-apoptotic effects of Venetoclax on CLL cells.

B cells purified from peripheral blood of CLL cells were treated with either 100 µM GroPIns or 3.5 nM Venetoclax, or a combination of both, for 24 h at 37°C. Our results show the enhanced apoptosis on CLL cells subjected to the combined treatment, compared to single treatments (**Fig. 6**).

Moreover, combined treatment not only enhanced not only expression (**Fig. 6B**), but also activation of Bax (**Fig. 6C**) in CLL cells, compared to single treatments. These results suggest a synergic pro-apoptotic activity of GroPIns and Venetoclax on CLL cells.

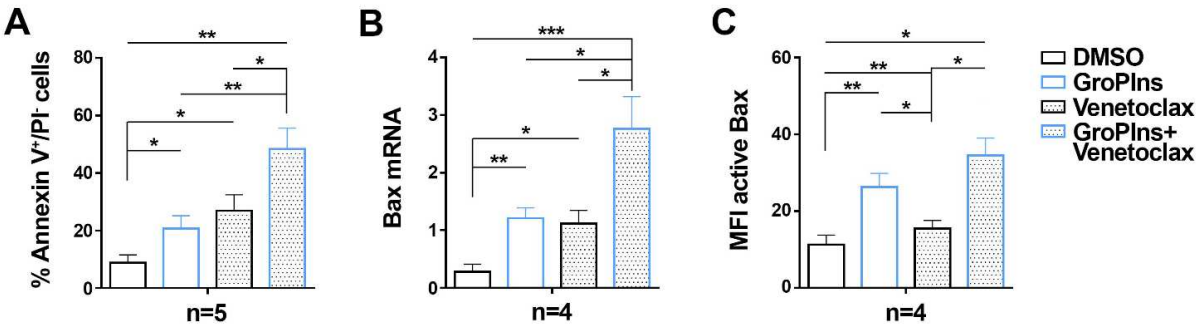

Figure 6. GroPIns enhances the pro-apoptotic activity of Venetoclax in CLL cells. (A) Flow cytometric analysis of the percentages of Annexin V^+/PI^- cells in B cells from CLL (n=5) treated with either 100 µM GroPIns or 3.5 nM Venetoclax or the combination of both for 24 h at 37°C. **(B)** qRT-PCR analysis of Bax mRNA in B cells from CLL (n=4) and treated as in (A). **(C)** Flow cytometric analysis of active Bax in CLL B cells (n=4) and treated for 20 min at 37°C with either 100 µM GroPIns or 3.5 nM Venetoclax or the combination of both. Mean ± SD. ANOVA one-way test, Multiple Comparison. $p \leq 0.001$, ***; $p \leq 0.01$, **; $p \leq 0.05$, *.

Part I

DISCUSSION

Apoptosis is a physiological mechanism which is essential for tissue development and homeostasis, as well as for the prevention of tumorigenesis.[10] The escape from the apoptotic program is one of the hallmarks of cancer and correlates with clinical resistance to therapies.[54]

In CLL, a profound imbalance in the expression of Bcl-2 family members towards the anti-apoptotic ones leads to the accumulation of CLL cells in secondary lymphoid organs.[8] The anti-apoptotic protein Bcl-2, whose expression is increased in CLL due to the deletion of miR-15 and miR-16, is considered a therapeutic target for CLL treatment.[12] Notably, Venetoclax, a BH3-mimetic drug capable of mimicking the activity of the physiological antagonists of Bcl-2 to induce apoptosis, has been approved for the treatment of relapsed/refractory CLL.[55]

The improved tolerability of targeted agents like Venetoclax has led to a decrease in the use of chemotherapeutic drugs such as Fludarabine and cyclophosphamide. Several studies are investigating the possibility of combining Venetoclax with Ibrutinib and monoclonal antibody anti-CD20. This combination could provide higher response rates compared to Venetoclax alone.[56,57] However, some CLL patients develop resistance to Venetoclax due to the acquisition of Bcl-2 mutations.

The altered apoptosis in CLL cells also depends on the reduced expression of Bax, a pro-apoptotic protein of the Bcl-2 family.[8] Following pro-apoptotic signals, Bax activation leads to the permeabilization of the mitochondrial membrane, releasing the apoptotic factor cytochrome *c* and promoting cell death.[58] A decrease in the Bcl-2/Bax ratio is associated with increased sensitivity to cytotoxic drugs in *vitro* and an improved response to treatment in CLL patients. Drugs clinically used to treat different types of cancer indirectly impact the expression and activation of Bax, including Fludarabine[51,59] and Venetoclax.[60] In this thesis, it has been demonstrated that, by enhancing both expression and activation of Bax, GroPIns promotes CLL cell apoptosis. Additionally, a higher level of apoptosis was observed in CLL cells treated with the combination of GroPIns and Venetoclax.

Therefore, our results highlight a potential new combinatorial strategy aimed at enhancing the pro-apoptotic activity of Venetoclax with a natural and well-tolerated compound. This approach may overcome potential resistance mechanisms to Venetoclax when used as a single agent.[61]

In the last decade, several classes of small molecules capable of selectively activating Bax and inducing apoptosis have been identified.[62,63] For example, the compound SMBA1 induces

conformational changes in Bax by inhibiting Serine184 phosphorylation. This process facilitates Bax insertion into mitochondrial membranes, resulting in the release of cytochrome *c* and apoptosis in human lung cancer cells. SMBA1 potently suppresses lung tumor growth in *vivo* through apoptosis, selectively activating Bax without causing significant toxicity in normal tissues.[64] Recently, new SMBA1 analogous have been synthesized, showing promise in inhibiting the proliferation of breast cancer cells.[65] However, none of these molecules has been tested in CLL until now.

On the other hand, the small molecule BDA-366, known as an antagonist of the BH4-domain with therapeutic potential in lung cancer and multiple myeloma treatments, has been evaluated in CLL and Diffuse large B-cell lymphoma (DLBCL). Unfortunately, this small molecule exhibited selective toxicity towards both CLL and DLBCL and the mechanism underlying Bax activation by BDA-366 remains unknown.[58,66]

In this study, GroPIns has been identified as a naturally occurring molecule with the ability to bind to and activate Bax. This discovery positions GroPIns as an intriguing candidate for testing in neoplasms characterized by reduced expression and activity of Bax.

CLL cells, in addition to aberrant expression of anti-apoptotic molecules, exhibit high levels of intracellular phosphorylation due to the hyperactivation of downstream B-cell receptor kinases such as Lyn, Syk, Btk, PI3K, and AKT.[67,68] This condition is also mediated by the altered activity of phosphatases, including PTEN[69], PP2A[70], and SHIP-1[71], which exhibit reduced expression in leukemic cells.

It is interesting that SHP-1, a tyrosine phosphatase involved in regulating the proliferation, survival, and apoptosis of both hematopoietic and non-hematopoietic cells,[38] is expressed in CLL cells at levels comparable to healthy B cells.[72] However, the function of this phosphatase is disrupted by mechanisms mediated by the Src family kinase Lyn, which inhibits the pro-apoptotic activity SHP-1 by phosphorylating its S591 residue,[43] making it an interesting target for the development of new drugs.

Unfortunately, SHP-1 has proven to be a challenging target for the development of specific drugs. This is attributed to both the highly conserved and positively charged nature of its active site and the limited selectivity or membrane permeability of the majority of phosphatase inhibitors[73]. It has been previously reported that GroPIns interacts with SHP-1 in melanoma cells.[37] This interaction facilitates the recruitment of SHP-1 to invadopodia, where it plays a role in dephosphorylating crucial components of the actin polymerization pathways. This process leads to matrix invasion, effectively counteracting metastasis.[46] In this context, we demonstrated that treatment of CLL cells with GroPIns enhances SHP-1phosphorylation. Despite the molecular mechanism underlying the

GroPIns-dependent increase in SHP-1 phosphorylation remains unknown, we can hypothesize that the interaction between GroPIns and SHP-1 stabilizes SHP-1 in a conformation which facilitates its interaction with an unknown kinase, thereby promoting SHP-1 phosphorylation. Active SHP-1 in turn promotes the expression of Bax[42,74] through signaling pathways involving the MAP kinase p38[42] and the transcription factor STAT3.[74] Therefore, by promoting the phosphorylation and activation of SHP-1, GroPIns enhances Bax expression and facilitates apoptosis in CLL cells, highlighting the potential of GroPIns to overcome the apoptosis deficiencies observed in CLL cells.

Part II

Leukemic cell-secreted interleukin-9 suppresses cytotoxic T cell-mediated killing in Chronic Lymphocytic Leukemia

Part II

INTRODUCTION

1.1 Mechanisms of immune evasion in the TME

1.1.1 The PD-1/PD-L1 immune checkpoint axis

Since escape from immune response is one of the hallmarks of cancer, restoring anti-tumor immunity has recently emerged as an interesting field of study. Immune checkpoints, which are characterized by ligand-receptor pairs which control the activation of immune effector cells to maintain self-tolerance and prevent autoimmunity,[75] are relevant molecular targets in anti-tumor immunity.

Notably, the PD-1 receptor and its ligands PD-L1 (Programmed cell death ligand 1) and PD-L2 (Programmed cell death ligand 2) stand out as a key inhibitory pathway, crucial for sustaining a tolerant microenvironment.[76] The PD-1 receptor is expressed by many immune cell types, including $CD4^+$ and $CD8^+$ T cells, monocytes, NK and DCs cells, while the membrane glycoproteins PD-L1 and PD-L2 are expressed by both hematopoietic and non-hematopoietic cells.[77] Interestingly, PD-L2 exhibits a binding profile selective for both PD-1 and RGM-2 (Repulsive guidance molecule family member 2) receptors, and its expression is limited to specific cell types. In contrast, PD-L1 exclusively interacts with the PD-1 receptor with a three times higher binding affinity compared to PD-L2.[78]

Upon T lymphocyte recognition of the specific antigen presented on the surface of an antigen-presenting cell, the binding between PD-1 and PD-L1 enables an inhibitory pathway [79] which leads to the phosphorylation of ITIM (immunoreceptor tyrosine-based inhibition motif) and ITSM (immunoreceptor tyrosine-based switch motif) motifs, located in the cytoplasmic tail of PD-1. These phosphorylation events recruit phosphatases such as SHP-2, thereby inducing the dephosphorylation of TCR-proximal signaling molecules.[80]

Physiologically, the PD-1/PD-L1 axis regulates the extent of inflammation following antigen recognition by T cells.[81] In the TME, the interaction between PD-1 on tumor-infiltrating T lymphocytes and PD-L1 on tumor cells plays a crucial role in tumor progression and survival.[75]

PD-1 upregulation on $CD4^+$ and $CD8^+$ T cell subsets is well documented in CLL.[20] Peripheral blood T cells of CLL patients express high levels of PD-1 compared to healthy donors. Furthermore, proliferation centres in lymph nodes of CLL patients exhibit high density of $PD1^+$ T cells, which are in close contact with leukemic cells, and hence subjected to chronic stimulation.[82]

Chronic antigenic stimulation can lead to several progressive phenotypic and functional changes, which promote T cell exhaustion. These changes involve loss of proliferative capacity and reduced production of interleukin-2 (IL-2), tumor necrosis factor-alpha (TNF-α), and interferon-gamma (IFN-γ).[83] These alterations coincide with enhanced expression of PD-1, LAG-3, and CTLA-4.[18] Additionally, exhausted $CD8^+$ effector T cells display inhibited killing capacity, and hence impaired ability to form an immunological synapse.[22,23] On the other hand, CLL cells exploit aberrant PD-L1 expression to suppress T cell effector functions and induce an exhausted phenotype in T cells, thereby evading immune surveillance.

Indeed, treatment with Ibrutinib has been shown to decrease PD-1/PD-L1 expression, influencing T cell proliferation and exhaustion, with significant implications for disease outcome.[84]

These findings suggest that clarifying PD-1/PD-L1 axis and its pathway may be crucial to better understand the mechanisms underlying CLL cell survival in the TME, as well as their ability to evade immune response.

1.1.2 CTL-mediated killing of tumor cells

CTLs recognize antigenic peptides presented by major histocompatibility complex class I (MHC I) on the surface of target cells through their TCRs. This recognition allows the formation of the IS, a specialized structure crucial for tumor cell killing.[85]

IS formation requires the coordinated and timely reorganization of lots of surface and cytoplasmic molecules towards the interface between effector T cell and antigen-presenting cell. Among them the actin cytoskeleton stands out, which ensures CTL polarization towards the target cell and mediates transport of the MTOC (Micro Tubule-Organizing Centre) beneath it.[86,87] MTOC docking at the synapse promotes polarization of lytic granules, specialized vesicular compartments containing lytic enzymes such as perforin and granzymes, towards the synaptic interface through a microtubule-assisted transport. Lytic granule exocytosis at the synapse results in the focal release of their cytotoxic contents inside the synaptic cleft and promotes target cell death through apoptosis (**Fig. 7**).[88,89] It is noteworthy that tumor cells, among which CLL cells, suppress CTL anti-tumoral functions by expressing immunosuppressive surface ligands such as PD-L1, which in turn bind and activate the cognate inhibitory receptors on CTLs. This interaction alters IS formation and impairs polarized lytic granule secretion into the synaptic cleft, thereby strongly affecting tumor cell killing.[90,91] Additionally, these inhibitory axes impair polarized actin cytoskeleton polymerization as well as recruitment of key molecules, including TCR, to the IS, thereby strongly affecting TCR-dependent signal transduction and activation of CTL effector functions, eventually helping CLL cells to escape from CTL-mediated killing. [92]

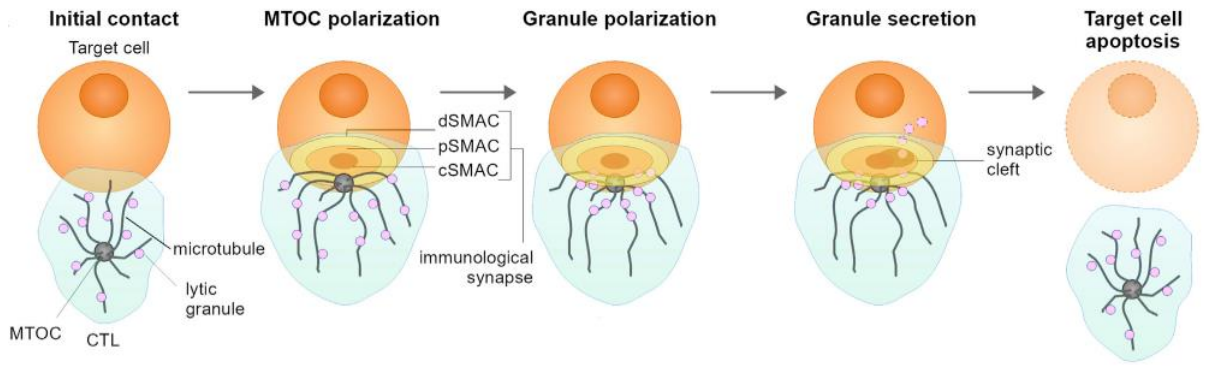

Figure 7. CTL-mediated killing of a target cell. After CTL recognition of a target cell the immunological synapse starts to assemble. This process leads to the translocation of the microtubule-organizing centre (MTOC) towards the synapse, followed by granule polarization to the MTOC. The release of lytic enzymes contained in the granules inside the synaptic cleft promotes the apoptosis of the target cell (adapted from Kabanova *et al*.[23]).

1.2 The molecular adaptor p66Shc and its deficiency in CLL cells

The Shc (Src homologous and collagen) family of molecular adaptors consists of four members: ShcA, ShcB, ShcC, ShcD, which are involved in signal transduction pathways that regulate growth, survival and response to oxidative stress.[93] Shc proteins exhibit a conserved structure, including a PTB domain (phosphotyrosine-binding domain) at the N-terminus, a central CH1 domain (collagen homologous region 1) and a SH2 domain (Src homology domain 2) at the C-terminus.

In mammals, ShcA is expressed in all tissues except for central nervous system, as three different isoforms of 46, 52 and 66 kDa (p46Shc, p52Shc and p66Shc).[94] The three isoforms are encoded by the same gene locus, although their expression is regulated by different promoters, one for the p52Shc and p46Shc isoforms and another for the p66Shc isoform.[95] p52Shc and p46Shc are constitutively and ubiquitously co-expressed. In contrast, p66Shc expression is tissue-specific and regulated by extracellular factors such as growth factors or hypoxic conditions, both physiologically and pathologically.[96]

p66Shc is distinguished from the other isoforms by its peculiar structure and physiological role. Indeed, it has an additional amino-terminal domain, called CH2, containing a phosphorylatable serine residue at position 36 (Ser36).[97] Moreover, it exists as two pools, one in the cytoplasm and the other in the mitochondrial intermembrane space,[98] where it translocates following phosphorylation on Ser36 by PKCβ (Protein Kinase C beta) and the MAPKs (Mitogen-Activated Protein Kinases) p38 and JNK, and where it interacts with cytochrome *c* thanks to the cytochrome-*c*-binding (CB) domain, a small region localized between the CH2 and PTB domains.[96]

In both T and B lymphocytes, p66Shc exhibits prominent pro-oxidant and pro-apoptotic activities,[99] which are mediated by integrated molecular mechanisms.[100] In mitochondria, binding of p66Shc to

cytochrome *c* interrupts the mitochondrial respiratory chain thereby producing ROS (Reactive Oxygen Species), which in turn mediate cytochrome *c* oxidation and loss of mitochondrial membrane potential. The subsequent formation of pores on the mitochondrial membrane promotes cytochrome *c* release, which induces apoptosis through the formation of the Apoptosome, followed by activation of the caspase cascade and of the apoptotic machinery.[98] Moreover, the pro-oxidant activity of p66Shc transcriptionally regulates the balance of pro- and anti-apoptotic members of the Bcl-2 family through still unknown molecular mechanisms.

The role of p66Shc as a master regulator of apoptosis in lymphocytes has significant implications in the pathogenesis of CLL.[101] In leukemic cells isolated from peripheral blood of CLL patients, p66Shc expression is significantly reduced compared to healthy B cells, showing a strong correlation with prognosis. Indeed, patients with lower p66Shc levels show a poorer prognosis.[101] Defective p66Shc expression in CLL cells leads to decreased expression of the anti-apoptotic members Bcl-2 and BCL2L1 and an upregulation of the pro-apoptotic members Bax and Bak, thereby favouring CLL cells survival.[101]

p66Shc also plays a key role in lymphocyte trafficking from the blood and lymph to lymphoid organs. By altering the balance of homing and egress receptors, p66Shc deficiency in CLL cells promotes leukemic cell retention in the pro-survival stromal niche of lymphoid organs.[100] In fact, leukemic cells show increased expression of the homing receptors CCR7 and CXCR4, at the same time expressing lower levels of the egress receptor S1PR1 (Sphingosine-1-Phosphate Receptor 1).[100,102] Altered lymphocyte trafficking allows leukemic cells to persist inside niches in lymphoid organs for longer than normal, where they are subject to pro-survival signals from the TME and are protected from the action of anti-cancer drugs.

The role of p66Shc in CLL pathogenesis has been well characterized in the mouse model of CLL Eμ-TCL1[103] and in the new mouse strain Eμ-TCL1/p66Shc$^{-/-}$.[104] In these mice, p66Shc deficiency leads to earlier onset and enhanced aggressiveness of the disease, with increased accumulation of leukemic cells in both lymphoid and non-lymphoid organs.[104] The enhanced ability of p66Shc-deficient leukemic cells to infiltrate nodal and extranodal sites was found to associate with increased secretion of the cytokine interleukin (IL)-9 by leukemic cells themselves that, in turn, drives the expression of homing chemokines by stromal cells of lymphoid organs.[49]

Secreted by T cells, mast cells, neutrophils, and NK cells,[105] IL-9 is not expressed by B lymphocytes. Its release has been found to modulate chemokine expression in non-immune cells, such as epithelial cells and astrocytes.[106,107] Aberrant or ectopic IL-9 expression was found in several neoplasias like pancreatic,[108] colorectal,[109] and non-small cell lung cancer.[110]

High IL-9 serum levels are associated with unfavourable CLL prognosis.[49,111] Interestingly, p66Shc deletion in leukemic Eμ-TCL1 cells or p66Shc deficiency in human CLL cells inversely correlates with IL-9 secretion.[49] IL-9 blockade in Eμ-TCL1/p66Shc$^{-/-}$ mice leads to a decrease in the nodal expression of homing chemokines, which correlates with decreased leukemic cell invasiveness.[49] Consistently, CLL patients with the highest IL-9 expression have an increased frequency of lymphadenopathy and splenomegaly, features that are associated with advanced disease and unfavourable prognosis.[2] Hence IL-9, by inducing chemokine expression in the lymphoid stroma, plays a key role in shaping the microenvironment, thereby contributing to the pathogenesis of CLL.

Part II

AIMS

CLL cells shape the TME by inducing the formation of a pro-survival and immunosuppressive niche which assists them escaping immune surveillance.[112] It is known that CLL cells, through contact-dependent interactions, implement several strategies to shape CTLs of the TME toward an exhausted phenotype, characterized by increased expression of exhaustion markers and inability to produce adequate levels of immune-activating cytokines, which both contribute to T cell dysfunctions.[90,91] This study aimed to investigate whether CLL cells also implement contact-independent mechanisms to induce CTL dysfunctions, namely through the release of soluble factors such as cytokines and chemokines, which integrate with direct cell-to-cell contacts to favour leukemic cell survival.

Part II

MATERIAL AND METHODS

2.1 CLL patients, healthy donors, mice and cell lines

The collection of peripheral blood samples from anonymous healthy donors was approved by the ethics committee (Siena University Hospital and Padova University Hospital) and performed after receiving signed informed consent according to institutional guidelines.

CLL diagnosis and mutational *IGHV* status were assessed as reported [2]. Peripheral blood samples were collected from 96 treatment-naïve CLL patients (>95% leukemic $CD5^+CD19^+/CD19^+$ cells) and 4 CLL patients subjected to Ibrutinib treatment (**Table 4**). Healthy control B cells were purified from 119 buffy coats. Transfections were previously described [100]. Non-randomized non blinded experiments were carried out on cells isolated from Eμ-TCL1, Eμ-TCL1/p66Shc$^{-/-}$ mice[103] and parental C57BL/6J mice. Disease development and overt leukemia achievement were assessed as reported [104]. In *vivo* treatment of Eμ- TCL1/p66Shc$^{-/-}$ leukemic mice with anti-IL-9 or isotype ctr antibodies was reported [49]. The Raji B lymphoblastoid cell line was previously described [113].

		CLL patients			
		# 1	# 2	# 3	# 4
IGHV status		Unmutated	Mutated	Mutated	Unmutated
TP53 status		Wild-type	Wild-type	Wild-type	Wild-type
TP53 status		Deleted and mutated	Mutated	Wild-type	Mutated
Follow-up[months]		32	21	33	19
WBC (n/mL)	Before Ibrutinib treatment	103000	74000	8560	138000
	Follow-up Ibrutinib treatment	40000	28000	5780	8410
Ly (n/mL)	Before Ibrutinib treatment	93000	68000	3900	130000
	Follow-up Ibrutinib treatment	36000	23000	2100	2200
Hb (g/L)	Before Ibrutinib treatment	127	150	134	95
	Follow-up Ibrutinib treatment	133	151	134	119
PLT (n/mL)	Before Ibrutinib treatment	530000	95000	67000	119000
	Follow-up Ibrutinib treatment	331000	80000	130000	166000
RAI Stage	Before Ibrutinib treatment	3	3	4	3
	Follow-up Ibrutinib treatment	0	1	0	1

Table 4. Clinical parameters of 4 CLL patients subjected to second line Ibrutinib treatment.

2.2 Conditioned supernatants and multiplex assays

Conditioned supernatants were generated and stored as reported [49]. Viability of healthy B cells and CLL cells used to generate conditioned supernatants was consistently >65% at 48 h versus ~85% immediately after purification. Mouse cytokines and chemokines were quantified by Bio-Plex Chemokine Panel Multiplex assay (BioRad). Data were acquired and analysed using Luminex-Magpix (BioRad).

2.3 Purification, activation and conditioning of $CD8^+$ cells

$CD8^+$ T cells isolated from spleens of C57BL/6J and Eμ-TCL1 by immunomagnetic sorting using Dynabeads™ Untouched Mouse CD8 Cells Kit were seeded on 6-well plates ($1.5x10^5$ cells/well) and incubated for 48 h with 2 ml supernatant conditioned by either leukemic or wild-type B cells.[112] 0.5 ng/ml recombinant murine IL-9 and 0.1 ng/ml of either control or anti-IL-9 mAb (**Table 5**) were added to culture media.

$CD8^+$ cells were isolated from peripheral blood of healthy donors and CLL patients by negative selection using the RosetteSep Human $CD8^+$ T Cell Enrichment Cocktail, following the manufacturer's instructions. On the same day (day 0), cells were stimulated in RPMI-HEPES medium (1×10^6/ml) (#R7388; Merck) supplemented with 10% BCS (#SH30072.03; GE Healthcare HyClone), 1% MEM nonessential amino acids (MEM NEAA; #11140050), and 50 U/ml recombinant human IL-2 with Dynabeads™ Human T-activator CD3/CD28. Media conditioned by either leukemic or wild-type B cells were immediately added to the activation medium, to a final 1:1 ratio (conditioned *vs* activation medium). 20 ng/ml recombinant human IL-9 or 0.5 ng/ml recombinant human IL-10, and 0.1 ng/ml isotype control, 1 ng/ml anti-IL-9 mAb or anti-IL10 mAb (**Table 5**), were added to culture media. 48 h after activation (day 2), beads were removed and CTLs were collected. For cytotoxicity and degranulation assays, CTLs were expanded in RPMI-HEPES supplemented with 10% BCS, 1% MEM NEAA, and 50 U/ml recombinant human IL-2 for additional 3 days, then further expanded for 2 days and collected at day 7.[6]

Reagents	Host	Clone	Source	Cat. n.	Concentration/dilution
CFSE	-	-	Thermo Fisher Scientific	C34554	1.5 µM
Propidium Iodide	-	-	Sigma-Aldrich	537059	0.5 µg/ml
Monensin	-	-	BioLegend	420701	2 µM
Fc-Block	rat	2.4G2	BD Biosciences	553141	1:50
PerCP-Cy5.5 IgM antibody	rat	RMM-1	BioLegend	406512	1:30
PE anti-mouse CD5 antibody	rat	53 - 7.3	BD Bioscience	553022	1:40
FITC anti-mouse CD19 antibody	rat	1D3	BD Bioscience	553785	1:40
PE anti-mouse CD8a (Ly-2) antibody	rat	53 – 6.7	BD Bioscience	553033	1:50
PE anti-human CD8a antibody	mouse	RPA-T8	BioLegend	301008	1:50
APC anti-human CD107a/LAMP1 antibody	mouse	H4A3	BioLegend	328619	1:160
Anti-PD1 antibody	rabbit	-	Novus	NBP1-77277	1:200
FITC anti-mouse CD45.1 antibody	-	A20	BioLegend	110705	1:50
FITC anti-human CD69 antibody	-	FN50	BioLegend	310904	1:100
Pe anti-huan CD25 antibody	-	BC96	BioLeged	302606	1:50
Percp-Cyanine anti-human CTLA-4 antibody	-	L3D10	BioLegend	349927	1:50
FITC anti-human LAG-3 antibody	-	11C3C65	BioLegend	369307	1:50
Fitc-Annexin V	-	-	BioLegend	640906	1:50
Anti-CD3ζ antibody	mouse	6B10.2	SantaCruz	Sc-1239	1:200
Anti- p-Tyr antibody	mouse	4G10	Cell Signaling	8954S	1:100
Anti-PCNT antibody	rabbit	-	Abcam	4448	1:200
Alexa Fluor 555 F-actin	-	-	Invitrogen	A34055	1:100
Alexa Fluor anti-mouse 488	goat	-	Thermo Fisher Scientific	A11001	1:80
Alexa Fluor anti-rabbit 555	goat	-	Thermo Fisher Scientific	A21428	1:80
Alexa Fluor anti-rabbit 647	goat	-	Thermo Fisher Scientific	A21236	1:400
Recombinant Mouse IL-9	-	-	R&D Systems	409-ML-010	0.5 ng/ml
Recombinant Human IL-9	-	-	R&D Systems	209-ILB-010	20 ng/ml
Recombinant Human IL-10 Protein	-	-	R&D Systems	217-ILB	0.5 ng/ml
Recombinant human IL-2	-	-	Miltenyi Biotech	130-097-745	50 Units/mL
IgG2B, isotype control antibody	Rat	141945	R&D Systems	MAB0061	0.1 ng/ml
Mouse IL-9 antibody	Rat	222622	R&D Systems	MAB4091-100	0.1 ng/ml
Human IL-9 antibody	Mouse	795908	R&D Systems	MAB2092	1 ng/ml
Human IL-10 antibody	Mouse	948505	R&D Systems	MAB9184	1 ng/ml
Neutralizing Human anti-PD-1 antibody	Rabbit		R&D Systems	AF1086	7.5 µg/ml
B-1a Cell Isolation Kit, mouse	-	-	Miltenyi Biotech	130-097-413	-
Dynabeads™ Untouched™ Mouse CD8 Cells Kit	-	-	Invitrogen	11417D	-
RosetteSep Human CD8+ T Cell Enrichment Cocktail	-	-	StemCell Technologies	15063	-
RosetteSep Human B Cell Enrichment Cocktail	-	-	StemCell Technologies	15064	-
Dynabeads Human T-activator CD3/CD28	-	-	Gibco	11132D	-
Ibrutinib	-	-	R&D Systems		10µM

Table 5. List of antibodies and reagents used in this study.

2.4 Immune synapse formation, immunofluorescence and analysis

Raji B cells (0.4×10^6 cells/100 µl) were loaded with 10 µg/ml Staphylococcal SAg A (SEA; Toxin Technologies, #AT101), B (SEB; Toxin Technologies, #BT202) and E (SEE; Toxin Technologies, #ET404) for 2 h to broadly cover the TCR Vβ repertoire, and labelled with 20 µM Cell Tracker Blue for 15 min.[6] Conjugates of CTLs with Raji B cells formed in the absence of SAgs were used as negative controls. Raji B cells were mixed with CTLs (1:1.5) and incubated for 15 min at 37°C. When required, 7.5 µg/ml anti-PD-1 neutralizing mAbs was added to the medium during conjugate formation. Samples were seeded onto poly-L-lysine (Merck, #P1274)-coated slides (ThermoFisher Scientific, #X2XER208B), fixed for 10 min in methanol at -20°C (for CD3ζ and pTyr staining) or for 15 min with 4% paraformaldehyde/PBS at room temperature (for PCNT and phalloidin staining) and permeabilized with 0.1% Triton, 1% BSA PBS. Cells were stained with primary antibodies overnight at 4°C, washed with PBS, incubated for 45 min at room temperature with Alexa Fluor 488- and 555-labeled secondary antibodies and mounted with 90% glycerol/PBS. Confocal microscopy was carried out on a Zeiss LSM700 (Carl Zeiss, Jena, Germany) microscope using a 63x/1.40 objective. Images were acquired with pinholes opened to obtain 0.8 µm-tick sections. Images were processed with Zen 2009 image software (Carl Zeiss, Jena, Germany). Immunofluorescence analyses were performed using ImageJ software. Scoring of conjugates for accumulation of CD3ζ, p-Tyr or F-actin at the IS, or for centrosome (PCNT) juxtaposition to the IS membrane, was performed as reported [6,114]. Recruitment indexes and quantification of the relative distances (µm) of the centrosome (PCNT staining) from the centre of the contact site with the APC were calculated using ImageJ.[6,114] Antibodies used for immunofluorescence microscopy are listed in **Table 5**.

2.5 Degranulation and Cytotoxicity assays

For degranulation assays,[6] Raji B cells were incubated with 1.5 µM carboxyfluorescein diacetate succinimidyl ester (CFSE; #C34554; Thermo Fisher Scientific) dissolved in PBS for 8 min at room temperature. CFSE-stained Raji B cells (0.025×10^6) were pulsed with 1 µg/ml SAgs for 1 h in serum-free AIMV medium (#12055-091; Gibco), then mixed with CTLs, at the ratios of 1:2.5, 1:5 and 1:10 (APC:CTL ratio) in 50 µl AIMV medium containing APC-labeled anti-human CD107a (LAMP1; BioLegend) mAb for 1 h. Monensin (BioLegend) was then added and cells were further incubated for further 3 h at 37°C. Unpulsed CFSE-stained Raji B cells were used as negative control. Then cells were washed, resuspended in cold PBS and acquired using a GUAVA flow cytometer (Merck Millipore).

For cytotoxicity assays,[6] Raji B cells (0.025×10^6) were stained with 1.5 µM CFSE; (#C34554; Thermo Fisher Scientific) 8 min at room temperature in PBS and then pulsed with 2 µg/ml SAgs for 1 h in serum-free AIMV medium. Unpulsed CFSE-stained Raji B cells were used as negative control. CTLs collected at day 7 were added to Raji B cells at different ratios (1:2.5, 1:5 and 1:10 APC:CTL ratio) in 50 µl AIMV medium and incubated at 37°C for 4 h to evaluate target cell killing. Raji B cells pulsed and unpulsed with SAgs were used to set up control samples. Cells were then diluted to 200 µl with cold PBS and acquired using a GUAVA flow cytometer. Propidium Iodide (PI, Sigma, #537059) was added before each acquisition to the final concentration of 20 µg/ml. Cytotoxicity (% target cell lysis) was calculated as follows: ($CFSE^+PI^+$ cells − $CFSE^+PI^+$ cells in control sample) × 100.

2.6 CLL cell Ibrutinib treatments and ELISA assays

Freshly isolated leukemic cells 453 purified from peripheral blood of 13 CLL patients were treated with 10 µM Ibrutinib for 48 h. DMSO was used as control. Samples were centrifuged and supernatants stored at -80°C. IL-9 was quantified by ELISA (Raybiotech).

2.7 In vivo Ibrutinib treatment of CLL patients

PB was collected from 4 CLL patients treated first line with chemoimmunotherapy. Patients from #1 to #3 received FCR (fludarabine 25 mg/ml plus cyclophosphamide 250 mg/ml administered on day 1-3 of cycles 1-6 and rituximab 375 mg/m2 on day 1 of cycle 1 and 500 mg/ml on day 1 of cycles 2-6). Patient #4 received BR (bendamustine 90 mg/m^2 administered on day 1-2 of cycles 1-6 and rituximab 375 mg/m^2 on day 1 of cycle 1 and 500 mg/ml on day 1 of cycles 2-6). These treatments were started at disease progression according to iwCLL criteria[2]. At disease relapse all patients were managed with Ibrutinib 420 mg once a day.[21] From each patient, PB samples were collected the starting day of Ibrutinib treatment and during follow-up.[2,21]

2.8 RNA purification, gene expression profiling, qRT-PCR

RNA was extracted from samples by using the RNeasy Plus Mini Kit (Qiagen) according to the manufacturer's instructions, and RNA purity and concentration were measured using QIAxpert (Qiagen). Single strand cDNAs were generated using the iScriptTM cDNA Synthesis Kit 28 (Bio-Rad), and qRT-PCR was performed using the SsoFastTM EvaGreenR supermix kit (Bio-Rad) and specific pairs of primers listed in **Table 6**. Samples were run in triplicate on 96-well optical PCR plates (Sarstedt AG, Nümbrecht, Germany). The relative gene transcript abundance was determined on triplicate samples using the ΔΔCt method and normalized to either HPRT1 (human-derived

samples) or GAPDH (mouse-derived samples). RNA from mouse-derived leukemic cells was subjected to gene array profile analysis as describe [49].

Gene	Forward 5'-3'	Reverse 5'-3'
Human IL-9	ACCAGACCATGCTTCAGTGA	TCTTCAGAAATGTCAGCGCG
Human IL-10	TGCCTTCAGCAGAGTGAAGA	GGTCTTGGTTCTCAGCTTGG
Human p66Shc	TCCGGAATGAGTCTCTGTCA	GAAGGAGCACAGGGTAGTGG
Human CCL22	ACTGCACTCCTGGTTGTCCT	CGGCACAGATCTCCTTATCC
Human CCL24	GGAGTGGGTCCAGAGGTACAT	CAGGTGGTTTGGTTGCCAG
Human HPRT1	AGATGGTCAAGGTCGCAAG	GTATTCATTATAGTCAAGGGCATATC
Mouse PD-1	CATGCCCAGGTACCTCAGTT	GAACCCAACTCCAGGACAGA
Mouse p66Shc	TGAGTTGGGAGAGCAGAGGT	CTCATTCCGAAGTGGGTTGT
Mouse IL-9	CTTGCCTGTTTTCCATCGGG	CACGGCACCAGGAAAGAAAA
Mouse GAPDH	AACGACCCCTTCATTGAC	TCCACGACATACTCAGCAC

Table 6. List of primers used in this study

2.9 Flow cytometry and viability assays

Leukemic cell immunophenotyping was performed as described.[104] Spleen slices were disgregated on 70-µm cell strainers (BioSigma). Cell viability was measured by flow cytometric analysis of 1×10^6 B cells co-stained with FITC-labeled Annexin V and Propidium iodide. Flow cytometry was performed using Guava Easy-Cyte cytometer (Millipore).

2.10 Statistical analyses

One-way and two-way ANOVA tests with post-hoc Tukey correction and multiple comparisons were used to compare multiple groups. Mann-Whitney rank-sum and paired t-tests were performed to determine the significance of the differences between two groups. Power and sample size estimations were performed using G*Power. Statistical analyses were performed using GraphPad Prism. *P* values <0.05 were considered significant. Sample size, determined on the basis of previous experience in the laboratory, and replicate number for each experimental group/condition are indicated in the figure legends.

Part II

RESULTS

3.1 Soluble factors released by CLL cells enhance PD-1 expression in CTLs and suppress their ability to assemble functional ISs

CTLs from CLL patients show an exhausted phenotype, with impaired ability to form the IS and kill target cells.[91,92] Accordingly, we observed enhanced expression of the exhaustion markers PD-1, CTLA-4 and LAG-3 in $CD8^+$ cells from CLL patients compared to healthy $CD8^+$ cells (**Fig. 8A, 8B**). We asked whether the CLL cell secretome participates in CTL exhaustion. $CD8^+$ cells immunopurified from healthy donors were differentiated to CTLs[115] and cultured for 48 h in the presence of complete culture medium alone or media conditioned by either healthy B cells or leukemic cells from CLL patients (**experimental workflow in Fig. 9A**). Under these experimental conditions healthy $CD8^+$ cells showed an exhausted phenotype, with enhanced expression of PD-1, CTLA-4 and LAG-3 (**Fig. 8C - 8E**).

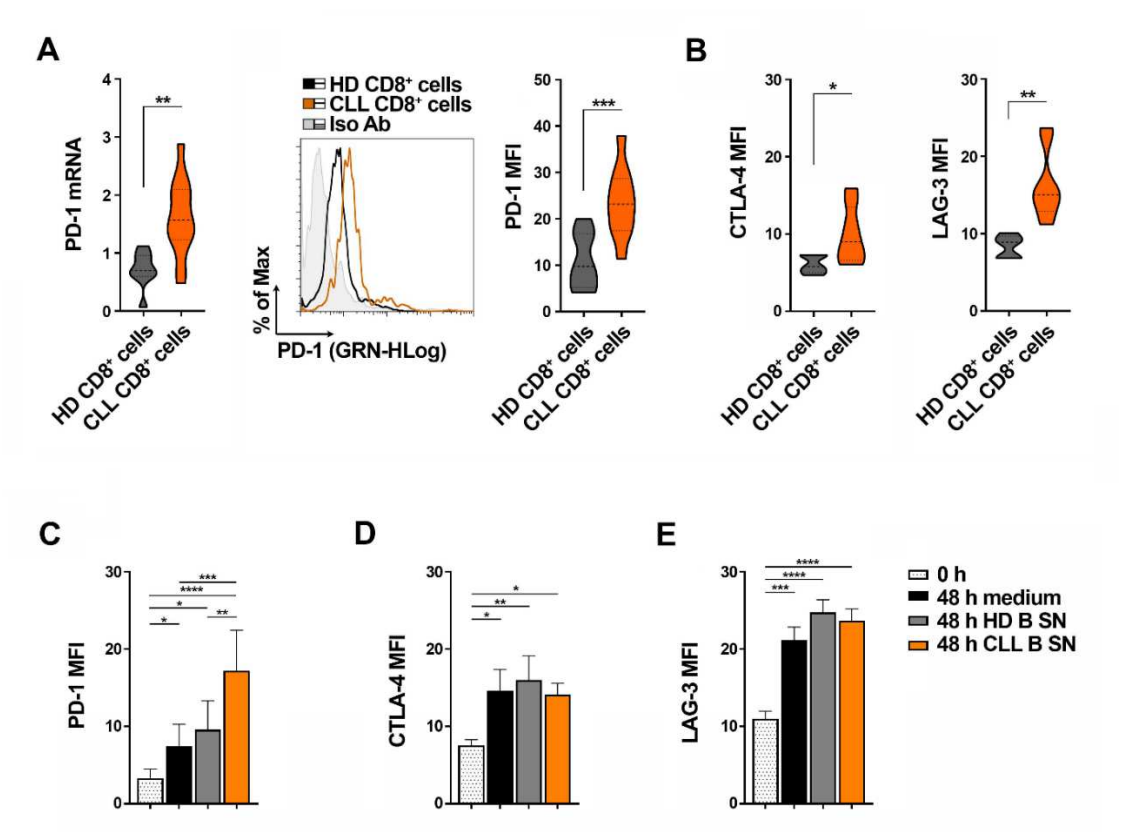

Figure 8. Expression of the exhaustion markers in $CD8^+$ cells from CLL patients compared to healthy $CD8^+$ cells A. qRT-PCR analysis of mRNA (*left*) and flow cytometric analysis of surface expression (*right*)

of PD-1 in $CD8^+$ cells purified from PB of healthy donors ($n \geq 8$) or CLL patients ($n \geq 10$). The flow cytometric histogram shows PD-1 staining in $CD8^+$ cells from a representative healthy donor and a representative CLL patient. The relative gene transcript abundance was determined on triplicate samples using the ΔΔCt method and normalized to HPRT1. **B.** Flow cytometric analysis of surface expression of CTLA-4 (*left*) and LAG-3 (*right*) in $CD8^+$ cells purified from PB of healthy donors ($n \geq 5$) or CLL patients ($n \geq 5$). **C-E**. Flow cytometric analysis of surface expression of PD-1 (*left*), CTLA-4 (*middle*) and LAG-3 (*right*) in $CD8^+$ cells purified from PB of healthy donors ($n \geq 3$), either immediately after purification (0 h) or activated for 48 h in complete culture medium or in the presence of media conditioned by healthy B cells / B cells purified from CLL patients. (A, B: Mann-Whitney Rank Sum test; C-E: Ordinary one-way ANOVA test ****, $p \leq 0.0001$; ***, $p \leq 0.001$; **, $p \leq 0.01$; *, $p \leq 0.05$.

Of note, the expression of PD-1 was significantly enhanced in healthy CTLs cultured in CLL cell-conditioned media compared to CTLs cultured in healthy B cell-conditioned media, but not that of CTLA-4 and LAG-3 (**Fig. 9B, 9C and Fig. 8C - 8E**), indicating that leukemic cells indirectly suppress CTL function by releasing soluble factors that promote their exhaustion by enhancing PD-1 expression. CLL cells suppress the ability of T cells to form functional ISs through cell-to-cell inhibitory contacts.[21,92] The contact-independent enhancement in PD-1 expression in CTLs cultured in conditioned media of CLL cells suggests that soluble CLL-derived factors may also contribute to the IS abnormalities. Healthy $CD8^+$ cells were cultured for 48 h in the presence of healthy B cell- or CLL cell-conditioned media and conjugated with Raji cells pulsed with a mixture of the Staphylococcal enterotoxins A, B and E (SAgs). CLL cell conditioned media significantly impaired IS assembly, as shown by the decreased frequency of conjugates displaying tyrosine phosphoprotein (pTyr), TCR/CD3 and F-actin staining at the CTL/APC interface and the impairment in their synaptic accumulation (**Fig. 9D - 9F**). Additionally, centrosome polarization, which is essential for lytic granule delivery to the target cell, was impaired under these conditions, as assessed by measuring the frequency of conjugates displaying centrosome localization beneath the IS membrane and its distance from the IS centre (**Fig. 9G**). These results suggest that in *vivo* $CD8^+$ cell conditioning exacerbates their inability to form the IS, likely through the combination of indirect mechanisms, mediated by CLL-derived soluble factors, and direct interactions involving multiple surface receptor-ligand inhibitory pairs.[91]

To test the outcome of these defects on CTL-mediated killing, healthy donor $CD8^+$ cells were activated in the presence of healthy or leukemic cell-conditioned media. After 7 days CTLs were incubated with CFSE-labelled SAg-pulsed Raji cells for 4 h, followed by propidium iodide staining and flow cytometric analysis. Consistent with the IS defects, CLL-conditioned media suppressed the ability of CTLs to kill target cells (**Fig. 9H**). Moreover, they significantly impaired CTL degranulation, as assessed by measuring the percentage of $CD8^+$ cells expressing at their surface the lytic granule marker LAMP-1 (**Fig. 9I**).

By counteracting TCR-dependent signaling, PD-1 prevents CTLs from forming functional ISs.[92,116] To assess whether PD-1 overexpression induced in healthy CTLs by CLL conditioned media is causal to their IS assembly defects, PD-1 neutralizing antibodies were added to CTLs cultured as in **figure 9A**, immediately prior to conjugate formation with SAg-pulsed Raji cells. PD-1 neutralization reverted the IS-suppressive effect of CLL cell conditioned media (**Fig. 9L**). Hence, leukemic cells indirectly control CTL exhaustion by secreting soluble factors that enhance PD-1 expression, which in turn impairs the ability of CTLs to form functional ISs and kill target cells.

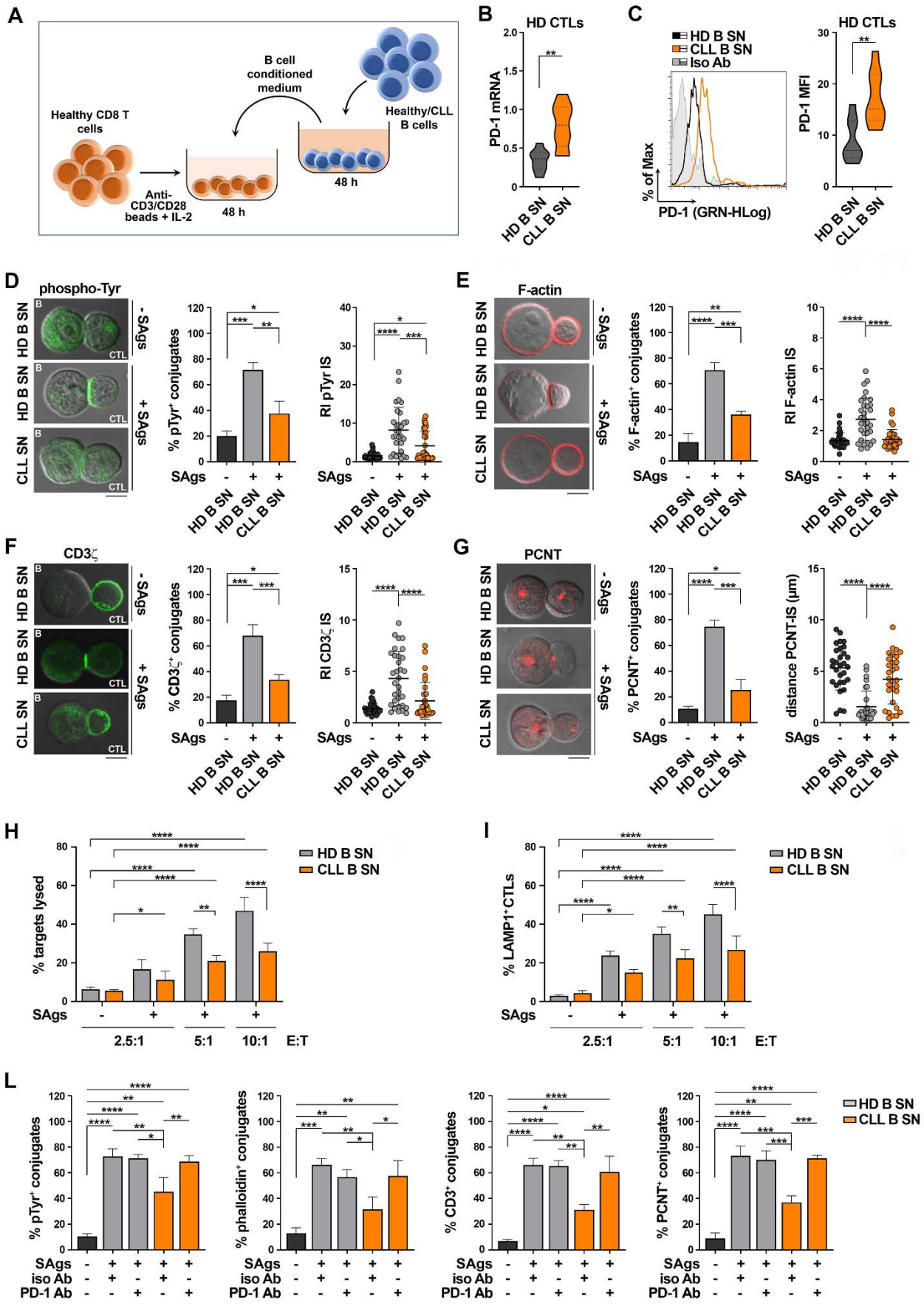
A
Healthy CD8 T cells
Anti-CD3/CD28 beads + IL-2
48 h
B cell conditioned medium
Healthy/CLL B cells
48 h
B
HD CTLs
PD-1 mRNA
HD B SN
CLL B SN
C
HD B SN
CLL B SN
Iso Ab
% of Max
PD-1 (GRN-HLog)
HD CTLs
PD-1 MFI
D
phospho-Tyr
HD B SN
CLL SN
- SAgs
+ SAgs
CTL
% pTyr+ conjugates
RI pTyr IS
SAgs
E
F-actin
% F-actin+ conjugates
RI F-actin IS
F
CD3ζ
% CD3ζ+ conjugates
RI CD3ζ IS
G
PCNT
% PCNT+ conjugates
distance PCNT-IS (µm)
H
% targets lysed
HD B SN
CLL B SN
2.5:1
5:1
10:1
E:T
I
% LAMP1+ CTLs
L
% pTyr+ conjugates
% phalloidin+ conjugates
% CD3+ conjugates
% PCNT+ conjugates
iso Ab
PD-1 Ab

Figure 9. Soluble factors released by CLL cells enhance PD-1 expression on CTLs and suppress their ability to form functional ISs. A. Workflow for CTL generation from $CD8^+$ cells purified from buffy coats of healthy donors and their treatment with media conditioned by either healthy B cells or B cells purified from CLL patients. **B, C.** qRT-PCR analysis of mRNA (**B**) and flow cytometric analysis of surface (**C**) expression of PD-1 in $CD8^+$ cells purified from buffy coats, stimulated with anti-CD3/CD28 mAb-coated beads + IL-2 for 48 h (CTLs), in the presence of conditioned media. A representative flow cytometric histogram is shown (n buffy coats from healthy donors = 9). **D-G.** Immunofluorescence analysis of pTyr (**D**), F-actin (**E**), CD3ζ. (**F**), and PCNT (**G**) in CTLs activated as in (**A-C**), mixed with Raji cells (APCs) either unpulsed or pulsed with a combination of SEA, SEB, and SEE (SAgs), and incubated for 15 min at 37°C. Data are expressed as % of 15-min SAg-specific conjugates harboring staining at the IS (≥50 cells/sample, n independent experiments = 3). Representative images (medial optical sections) of the T cell:APC conjugates are shown. Scale bar, 5 μm. **D-F**, *right panels.* Relative fluorescence intensity of pTyr (**D**), F-actin (**E**), and CD3ζ (**F**) at the IS (recruitment index, RI; 10 cells/sample, n independent experiments = 3). ***G***, *right panel*. Measurement of the distance (μm) of the centrosome (PCNT) from the CTL:APC contact in conjugates formed as above (10 cells/sample, n independent experiments = 3). **H**. Flow cytometric analysis of target cell killing by CTLs cultured for 7 days in conditioned media, using Sag loaded CFSE-labelled Raji cells as targets at an E:T cell ratio 2.5:1, 5:1 and 10:1. Cells were cocultured for 4 h and stained with propidium iodide prior to processing for flow cytometry. Analyses were carried out gating on $CFSE^+/PI^+$ cells. The histogram shows the percentage (%) of target cells lysed (n≥785 3) **I**. Flow cytometric analysis of degranulation of CTLs cultured for 7 days as in (**H**), then cocultured with CFSE stained SAg-loaded Raji cells for 4 h. The histogram shows the percentage (%) of $LAMP1^+$ CTLs, measured gating on the CSFE-negative population (n independent experiments ≥3). **L.** Immunofluorescence analysis of pTyr, F-actin, CD3ζ, and PCNT in CTLs activated for 48 h in the presence of conditioned media, mixed with Sag loaded Raji cells (APCs), and incubated for 15 min at 37°C. Immediately before mixing the cells, either isotype control (iso Ab) or anti-PD-1 (PD-1 Ab) antibodies were added to CTLs. Data are expressed as % of 15-min SAg-specific conjugates harboring pTyr, F-actin, CD3ζ, and PCNT staining at the IS (≥50 cells/sample, n independent experiments =3). Data are expressed as mean ± SD. (B-L): Mann Whitney Rank Sum Test (B, C); one-way Anova test (D-L). ****, $p \leq 0.0001$; ***, $p \leq 0.001$; **, $p \leq 0.01$; *, $p \leq 0.05$.

3.2 The p66Shc expression defect in CLL cells contributes to their soluble PD-1-elevating and IS-disrupting activity

CLL cells have a profound defect in the expression of the pro-oxidant adaptor p66Shc, with the lowest levels in leukemic cells from patients with unfavourable prognosis.[117] This defect, which translates into a redox imbalance,[96,98] impinges on the expression of a number of CLL-critical genes, including genes encoding lymphoid homing and egress receptors, and cytokines such as IL-9.[49] Since T cells from poor prognosis patients show higher PD-1 levels compared to favourable prognosis patients,[91] we asked whether the p66Shc defect in CLL cells may impact on the expression of the soluble factors that promote PD-1 expression in CTLs.

The mRNA levels of p66Shc in CLL cells inversely correlated with PD-1 mRNA and surface expression in patient-matched $CD8^+$ cells (**Fig. 10A**). This inverse correlation was also observed when healthy CTLs were cultured in media conditioned by CLL cells with different levels of residual p66Shc (**Fig. 10B**), suggesting the existence of an indirect p66Shc-dependent mechanism through which CLL cells regulate PD-1 expression in CTLs. To test this hypothesis, we reconstituted p66Shc expression in CLL cells by transient nucleofection (**Fig. 10C**). Media conditioned by CLL transfectants were used to culture healthy CTLs. p66Shc reconstitution

reverted the PD-1-enhancing (**Fig. 10D, 10E**) and IS-suppressive (**Fig. 10F**) activities of CLL-conditioned media on CTLs. Hence the p66Shc defect in CLL cells modulates their secretome to promote PD-1 elevation and CTL suppression.

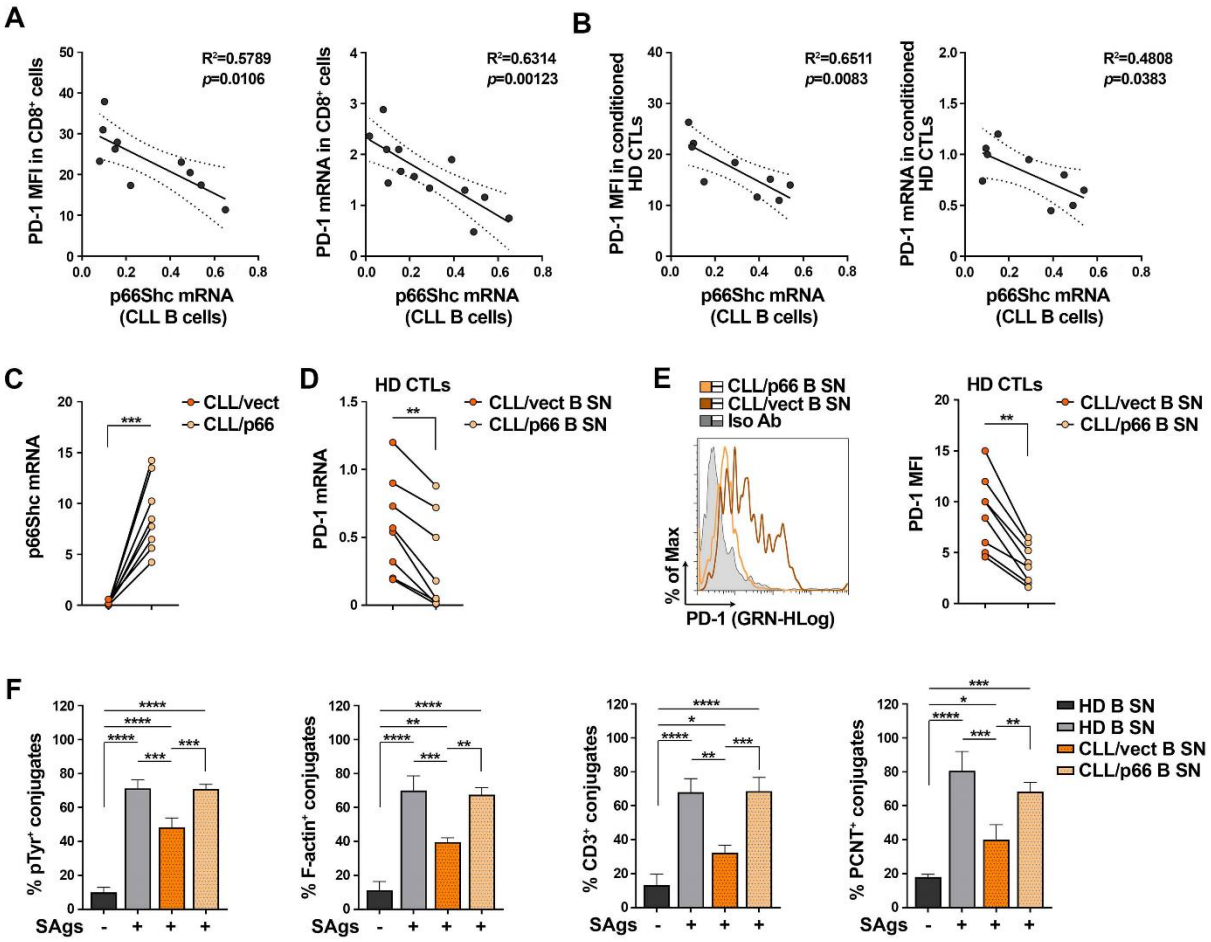

Figure 10. PD-1 overexpression induced in CTLs by CLL culture supernatants is caused by p66Shc deficiency. A. Correlation between either surface (MFI) or mRNA levels of PD-1 in $CD8^+$ cells isolated from CLL patients and the mRNA levels of p66Shc in B cells purified from the respective CLL patients (n CLL patients ≥ 10). **B**. Correlation between either surface (MFI) or mRNA levels of PD-1 in healthy CTLs activated for 48 h in media conditioned by CLL-B cells, and the mRNA levels of p66Shc in B cells purified from the respective CLL patients used to generate conditioned media (n=9). **C.** qRT-PCR analysis of p66Shc mRNA in B cells purified from CLL patients (n=8) and transfected with either empty (CLL/vect) or p66Shc-encoding (CLL/p66) vectors. **D, E.** qRT-RT PCR analysis of mRNA (**E**) and flow cytometric analysis of surface (**F**) expression of PD-1 in CTLs from heathy donors (n=8), activated for 48 h in the presence of media conditioned by CLL B cell transfectants. Representative flow cytometric histograms are shown. **F.** Immunofluorescence 810 analysis of pTyr, F-actin, CD3ζ, and PCNT in CTLs activated in media conditioned by CLL-B cell transfectants, mixed with SAg-loaded Raji cells (APCs), and incubated for 15 min at 37°C. Data are expressed as % of 15-min Sag specific conjugates harboring pTyr, F-actin, CD3ζ, and PCNT staining at the IS (≥ 50 cells/sample, n independent experiments=3). Data are expressed as mean±SD (C-F): paired t test (C, E); one-way ANOVA test (F). ****, $p \leq 0.0001$; ***, $p \leq 0.001$; **, $p \leq 0.01$; *, $p \leq 0.05$.

3.3 p66Shc deficiency in leukemic cells from Eμ-TCL1 mice enhances their soluble PD1- elevating activity on $CD8^+$ cells

In agreement with a previous report,[118] we found PD-1 overexpressed in $CD8^+$ cells isolated from lymph nodes of Eμ-TCL1 mice, the mouse model of CLL,[103] compared to their wild-type counterparts (**Fig. 11A, 11B**). PD-1 expression increased during disease progression, as assessed by flow cytometric analysis of $CD8^+$ cells from Eμ-TCL1 mice with either mild (20-39% leukemic cells in PB, 1-2×10^7 WBC/ml PB) or overt (>40% leukemic cells in PB, >2×10^7 WBC/ml PB) leukemia (**Fig. 11C**). p66Shc expression defect in leukemic cells from Eμ-TCL1 mice becomes more pronounced during disease progression,[104] and contributes to disease development and aggressiveness.[104,49,118] Consistent with the data obtained in CLL cells, PD-1 mRNA and surface expression in $CD8^+$ cells inversely correlated with the levels of residual p66Shc mRNA in leukemic Eμ-TCL1 cells (**Fig. 11D**). We asked whether the suppressive activity of CLL cell-conditioned media was reproduced in Eμ-TCL1 mice. PD-1 expression was enhanced in lymph node $CD8^+$ cells purified from wild-type mice cultured in Eμ-TCL1 cell-conditioned media (**Fig. 11E**) (same experimental workflow as for human $CD8^+$ cells, **Fig. 9A**), indicating that, similar to human CLL, leukemic cells promote bystander $CD8^+$ cell exhaustion in Eμ-TCL1 mice through a contact independent mechanism. PD-1 expression further increased in healthy splenic $CD8^+$ cells cultured in media conditioned by leukemic cells from Eμ-TCL1/p66Shc$^{-/-}$ mice (**Fig. 11E**), which develop an aggressive disease.[104] Hence, leukemic cells from Eμ-TCL1 mice indirectly suppress $CD8^+$ cell functions by secreting soluble factors that enhance PD-1 expression in a p66Shc-dependent manner.

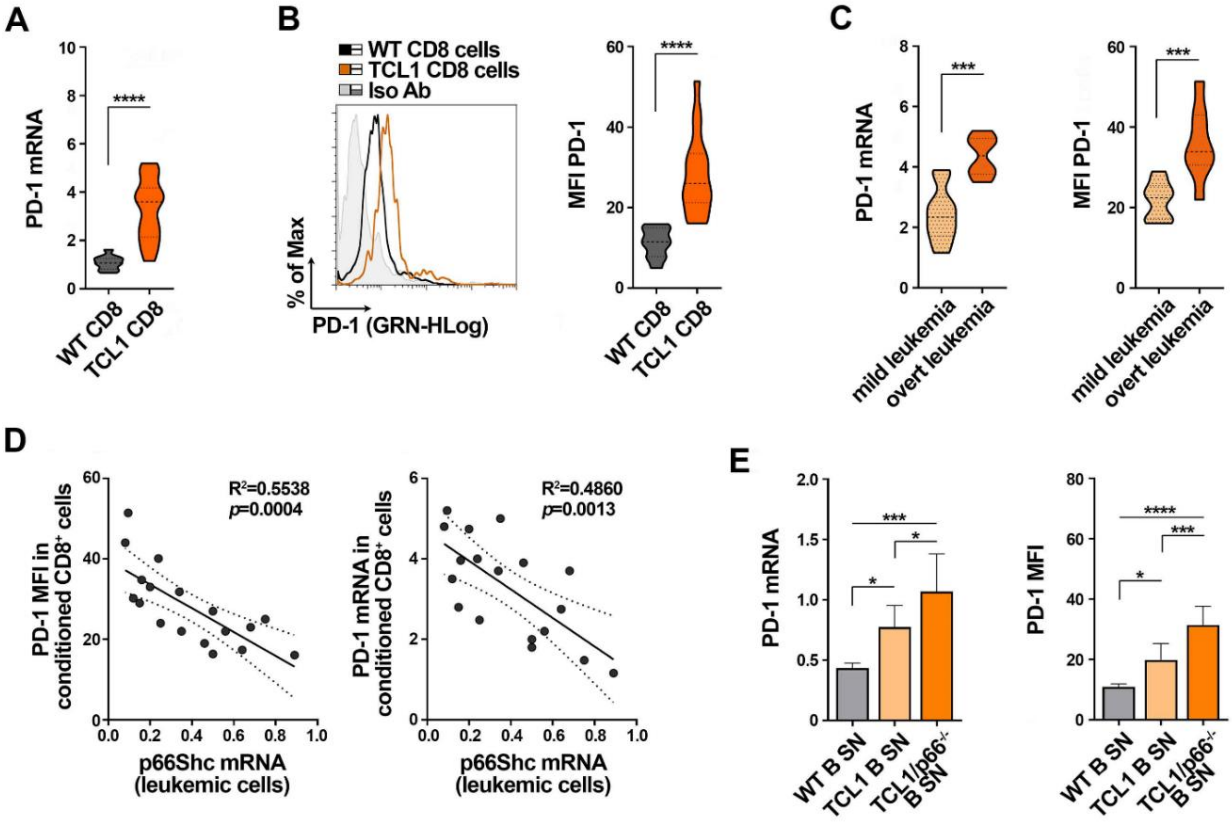

Figure 11. p66Shc deficiency in Eμ-TCL1 mice enhances the ability of leukemic cell to enhance PD-1 expression in CD8$^+$ cells. A, B. qRT-PCR analysis of mRNA (**A**) and flow cytometric analysis of surface (**B**) expression of PD-1 in CD8$^+$ cells isolated from lymph nodes of either wild-type (n = 10) or Eμ-TCL1 (n = 18) mice. Representative flow cytometric histograms are shown. **C**. mRNA expression of PD-1 in CD8$^+$ cells from lymph nodes of Eμ-TCL1 shown in (**A**) were subgrouped, according to disease stage, in mild leukemia (20-39% leukemic cells in PB, 1-2×10^7 WBC/ml PB, n Eμ-TCL1 mice = 10) and overt leukemia (>40% leukemic cells in PB, >2×10^7 WBC/ml PB, n Eμ-TCL1 mice = 8). **D**. Correlation between surface (MFI) or mRNA levels of PD-1 in CD8$^+$ cells isolated from lymph nodes of wild-type mice cultured in the presence of media conditioned by splenic B cells from Eμ-TCL1 mice, and the mRNA levels p66Shc in Eμ-TCL1 cells used to generate conditioned media (n wild-type mice=18). **E**. qRT-PCR analysis of PD-1 mRNA in CD8$^+$ cells isolated from spleens of wild-type mice (n=10), cultured in the presence of media conditioned by splenic B cells from either wild-type, Eμ-TCL1 or Eμ-TCL1/p66$^{-/-}$ mice (n independent experiments ≥5). Data are expressed as mean±SD (A, B, C, E): Mann Whitney Rank Sum test (A, B, C); one-way ANOVA test (E). ****, $p \leq 0.0001$; ***, $p \leq 0.001$; **, $p \leq 0.01$; *, $p \leq 0.05$.

3.4 p66Shc deficiency impinges on the cytokine landscape of CLL cells

CLL cell-derived IL-9 promotes the secretion of homing chemokines by stromal cells of the TME.[49] To identify leukemic cell-derived soluble factors with potential CTL-suppressive activity, we first quantified a panel of cytokines and chemokines released in media conditioned by splenic B cells from wild-type, Eμ-TCL1 or Eμ-TCL1/p66$^{-/-}$ mice by Multiplex ELISA. We identified soluble factors whose amounts were significantly increased in media conditioned by leukemic cells compared to their wild-type counterparts (**Fig. 12A**, **Table 7**), and selected the top candidates based on their significantly higher amounts in Eμ-TCL1 cell- *vs* wild-type B cell-conditioned media, and

Eμ-TCL1/p66$^{-/-}$ cell- *vs* Eμ-TCL1 cell-conditioned media. Moreover, we established a threshold of 100 ng/ml in media conditioned by wild-type cells.

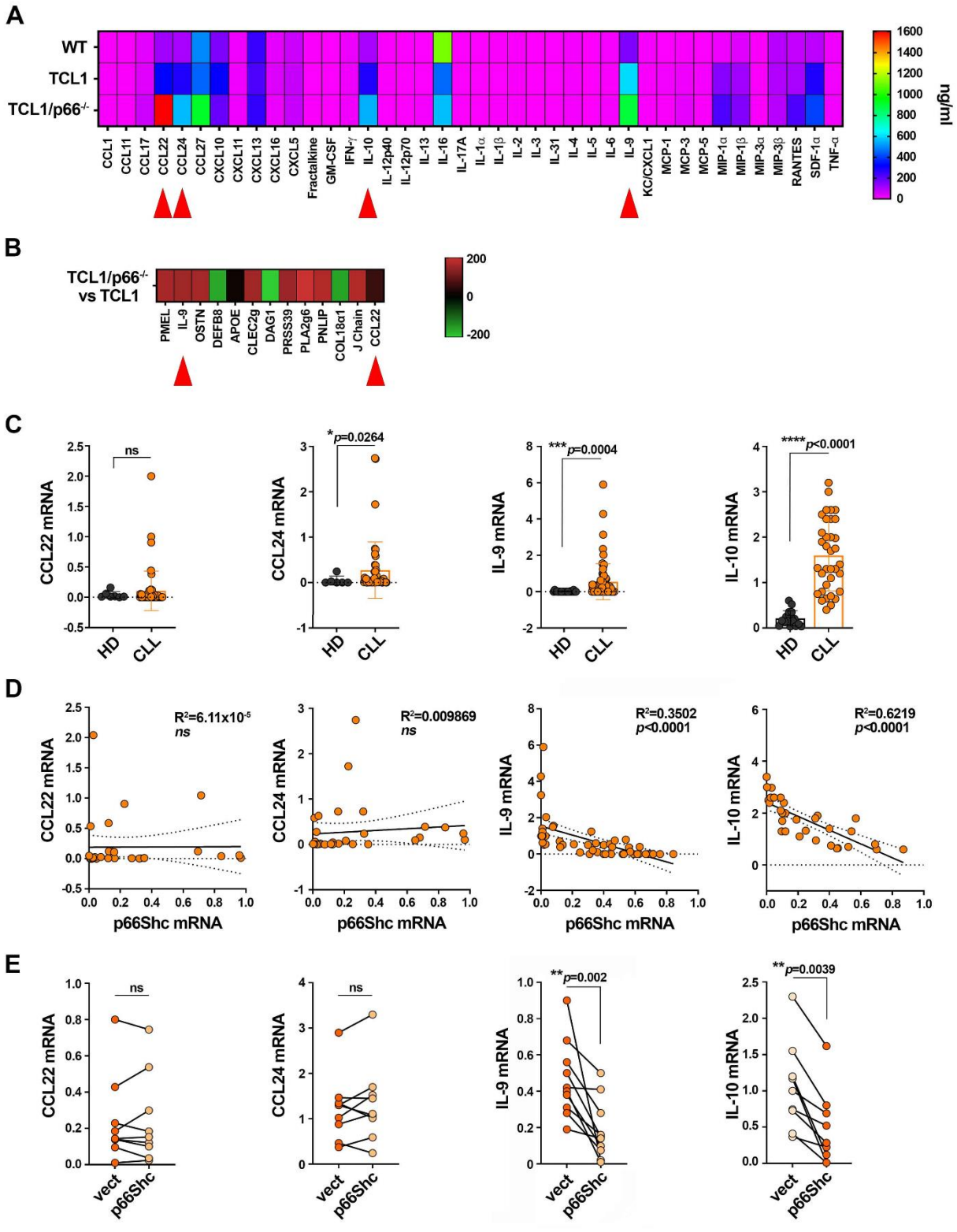

Figure 12. p66Shc deficiency impinges on the cytokine landscape of leukemic cells in Eμ-TCL1 mice and CLL. **A.** Heat map of the amounts of cytokines and chemokines in the culture supernatants of B cells

isolated from spleens of wild-type mice (WT; n=40), or leukemic cells purified from spleens of Eμ-TCL1 (TCL1; n=40) or Eμ-TCL1/p66$^{-/-}$ (TCL1/p66$^{-/-}$; n=40) mice and quantified by Multiplex ELISA. **B**. Heat map of transcripts from Affymetrix array analysis showing differential expression patterns between leukemic Eμ-TCL1 (TCL1, n=3) and Eμ-TCL1/p66Shc$^{-/-}$ (TCL1/p66$^{-/-}$, n=3) cells. Differential expression criteria: *p*-value < 0.05, estimated fold change > 2. Up-regulated and down regulated transcripts are shown in red and green, respectively. **C**. qRT-PCR analysis of mRNA expression of CCL22, CCL24, IL-9 and IL-10 in B cells purified from peripheral blood of healthy donors (n≥6) or CLL patients (n≥45). **D.** Correlation between mRNA levels of CCL22, CCL24, IL-9 or IL-10 and p66Shc mRNA levels in the respective CLL patients (n≥31). **E**. qRT-PCR analysis of mRNA expression of CCL22, CCL24, IL-9 and IL-10 in B cells purified from CLL patients (n=9) and transiently nucleofected with either empty (vect) or with p66Shc-expressing (p66Shc) vectors. Data are expressed as mean±SD (C, E); Mann Whitney Rak Sum test (C); Wilcoxon test (E). ****, $p \leq 0.0001$; ***, $p \leq 0.001$; **, $p \leq 0.01$; *, $p \leq 0.05$.

Among all soluble factors tested, only CCL22, CCL24, IL-9 and IL-10 met all our criteria. Of these, CCL22 and IL-9 were previously shown to be overexpressed by leukemic cells isolated from spleens of Eμ-TCL1/p66Shc$^{-/-}$ compared to Eμ-TCL1 mice (**Fig. 12B**, **Table 8** and [49]).

To translate these findings to the context of CLL, we quantified the selected candidates in B healthy and CLL cells by qRT-PCR. The levels of CCL24, IL-9 and IL-10 mRNAs were significantly higher in CLL cells compared to healthy B cells, while CCL22 expression was comparable to healthy B cells (**Fig. 12C**). As previously reported [49], the IL-9 mRNA levels inversely correlated with the p66Shc mRNA levels (**Fig. 12D**). This also applied to IL-10, but not to CCL22 or CCL24 (**Fig. 12D**). Moreover, p66Shc reconstitution in CLL cells by transient nucleofection led to a decrease in the mRNA of IL-9 (**Fig. 12E** and [49]) and IL-10, but not of CCL22 or CCL24 (**Fig. 12E**).

Protein	C57BL/6 SN ng/ml	TCL1 SN ng/ml	TCL1/p66$^{-/-}$ SN ng/ml	p-value TCL1 SN vs C57BL/6 SN	p-value TCL1/p66$^{-/-}$ SN vs C57BL/6 SN	p-value TCL1/p66$^{-/-}$ SN vs TCL1 SN
CCL1	2.57 ± 0.3	5.86 ± 3.5	5.41 ± 2.7	-	-	-
CCL11	3.11 ± 0.1	3.51 ± 0.7	3.21 ± 0.7	-	-	-
CCL17	33.16 ± 0.5	37.74 +/- 4.5	62.53 +/- 13.1	-	*p<0.05	*p<0.05
CCL22	**116.65 ± 50.98**	**324.23 ± 227.4**	**1605.74 ± 756.0**	***p<0.05**	****p<0.01**	***p<0.05**
CCL24	**106.54 ± 23.5**	**279.96 ± 147.0**	**555.44 ± 211.3**	****p<0.01**	*****p<0.001**	****p<0.01**
CCL27	492.53 ± 90.3	445.98 ± 32.8	912.95 ± 365.5	-	*p<0.05	*p<0.05
CXCL10	161.94 ± 6.6	315.49 ± 83.0	189.72 ± 48.68	*p<0.05	-	-
CXCL11	19.93 ± 0.3	17.50 ± 2.55	19.50 ± 1.3	-	-	-
CXCL13	247.50 ± 34.9	220.33 ± 74.9	256.45 ± 80.2	-	-	-
CXCL16	29.34 ± 7.5	40.55 ± 27.0	22.58 ± 15.8	-	-	-
CXCL5	62.87 ± 14.6	66.74 ± 15.1	69.97 ± 19.6	-	-	-
Fractalkine	4.89 ± 0.9	ND	6.32 ± 2.3	ND	-	ND
GM-CSF	0.28 ± 0.0	0.21 ± 0.1	0.55 ± 0.4	-	-	-
IFN-γ	20.47 ± 1.6	19.30 ± 6.0	17.05 ± 1.0	-	-	-
IL-10	**105.81 ± 12.4**	**279.37 ± 102.5**	**544.88 ± 154.5**	***p<0.05**	*****p<0.001**	***p<0.05**
IL-12 p40	3.05 ± 1.8	6.06 ± 5.0	1.68 ± 1.4	-	-	-
IL-12 p70	0.13 ± 0.05	0.15 ± 0.06	0.13 ± 0.04	-	-	-
IL-13	0.35 ± 0.18	1.37 ± 0.85	12.03 ± 7.4	-	**p<0.01	*p<0.05
IL-16	1113.91 ± 119.5	453.87 ± 257.6	561.02 ± 194.4	*p<0.05	-	-
IL-17A	0.03 ± 0.001	0.03 ± 0.002	0.02 ± 0.001	-	-	-
IL-1α	0.0028 ± 0.0004	0.0075 ± 0.003	0.005 ± 0.0008	**p<0.01	-	-
IL-1β	5.56 ± 0.9	2.0 ± 0.0	4.01 ± 2.8	-	-	-
IL-2	3.83 ± 0.3	3.28 ± 0.6	4.61 ± 0.9	-	-	-
IL-3	ND	ND	ND	ND	ND	ND
IL-31	1.72 ± 0.87	1.22 ± 0.68	1.23 ± 0.67	-	-	-
IL-4	10.26 ± 1.9	8.21 ± 1.1	11.68 ± 1.0	-	-	-
IL-5	ND	ND	ND	ND	ND	ND
IL-6	11.87 ± 1.0	7.16 ± 2.7	9.94 ± 5.0	-	-	-
IL-9	**161.01 ± 22.8**	**600.28 ± 176.3****	**890.48 ± 205.2**	****p<0.01**	*****p<0.001**	****p<0.01**
KC/CXCL1	8.48 ± 1.4	4.214 ± 1.1	5.23 ± 3.6	*p<0.05	-	-
MCP-1	1.1 ± 0.3	12.76 ± 11.1	5.2 ± 3.3	-	-	-
MCP-3	5.68 ± 0.5	20.11 ± 5.0	29.52 ± 3.9	*p<0.05	*p<0.05	-
MCP-5	ND	10.40 ± 2.9	4.03 ± 0.0	ND	ND	**p<0.01
MIP-1α	17.43 ± 5.0	147.41 ± 25.6	221.76 ± 50.4	**p<0.01	*****p<0.001**	****p<0.01**
MIP-1β	37.70 ± 11.3	116.66 ± 23.0	156.93 ± 55.0	**p<0.01	**p<0.01	*p<0.05
MIP-3α	6.48 ± 0.5	5.26 ± 1.3	7.35 ± 2.8	-	-	-
MIP-3β	87.04 ± 13.1	98.754 ± 51.9	87.148 ± 27.7	-	-	-
RANTES	73.92 ± 23.3	106.97 ± 85.4	223.28 ± 124.15	*p<0.05	**p<0.01	*p<0.05
SDF-1α	84.16 ± 34.3	283.48 ± 91.6*	401.05 ± 111.7*/**	*p<0.05	*p<0.05	**p<0.01
TNF-α	16.4 ± 0.7	14.05 ± 5.2	15.06 ± 3.9	-	-	-

Table 7. **p66Shc deficiency in Eμ-TCL1 mice correlates with enhanced secretion of CCL22, CCL24, IL-9 and IL-10 by leukemic cells.** List and concentrations (ng/ml) of the soluble factors released in the culture supernatants of either B cells purified from wild-type mice (n = 7) or leukemic cells purified from Eμ-TCL1 (TCL1, n = 15) and Eμ-TCL1/p66Shc$^{-/-}$ (TCL1/p66$^{-/-}$, n = 16) mice. The amounts of CCL22, CCL24, IL-9 and IL-10 (highlighted in bold) were significantly enhanced in Eμ-TCL1 and Eμ-TCL1/p66Shc$^{-/-}$ *vs* wild-

type supernatants, and in Eμ-TCL1/p66$^{-/-}$ *vs* Eμ-TCL1. (Student's t test). ***, $p \leq 0.001$; **, $p \leq 0.01$; *, $p \leq 0.05$.

Protein name	Gene symbol	Ref Seq	p-value (TCL1-P66$^{-/-}$ vs TCL1)	fold-change (TCL1-P66$^{-/-}$ vs TCL1)
Melanocyte protein	pmel	NM_021882	0.00226604	164.968
Interleukin 9	**IL9**	**NM_008373**	**0.00263432**	**158.872**
Osteocrin	ostn	NM_198112	0.0078197	161.911
Defensin beta 8	defb8	NM_153108	0.00971031	-156.532
Apolipoprotein E	apoe	NM_009696	0.0174238	22.271
C-type lectin domain family 2 member G	clec2g	NM_001168223	0.0210042	160.048
Dystroglycan 1	dag1	NM_001276481	0.0283007	-192.572
Inactive serine protease 39	prss39	NM_009355	0.0320975	152.112
85/88 kDa calcium-independent phospholipase A2	pla2g6	NM_001199023	0.0330742	200.803
Pancreatic triacylglycerol lipase	pnlip	NM_026925	0.0351441	175.732
Collagen alpha-1 (XVIII) chain	col18a1	NM_001109991	0.035647	-151.152
Immunoglobulin J chain	jchain	NM_152839	0.0398578	174.997
C-C motif chemokine 22	**CCL22**	**NM_009137**	**0.0467757**	**65.323**

Table 8. List of soluble molecules whose expression is significantly modulated in leukemic cells from Eμ-TCL1/p66Shc$^{-/-}$ vs Eμ-TCL1 mice. Fold change and *p* value of soluble factor expression extrapolated from Affymetrix array analysis showing differential expression patterns between leukemic Em-TCL1 (TCL1, n = 3) and Em-TCL1/p66Shc$^{-/-}$ (TCL1/p66$^{-/-}$, n = 3) cells. Differential expression criteria: *p*-value < 0.05, estimated fold change > 2. Differentially expressed genes are highlighted in bold.

3.5 IL-9 secreted by leukemic cells from CLL patients promotes PD-1 expression in CTLs

Based on these results, we assessed IL-9 and IL-10 as potential p66Shc-dependent, CTL suppressive soluble factors produced by CLL cells. We quantified surface PD-1 in healthy CTLs cultured with healthy or leukemic cell-conditioned media, in the presence of anti- IL-9 or anti-IL-10 neutralizing antibodies. Anti-IL-9 (**Fig. 13A**) but not anti-IL-10 (**Fig. 13B**) antibodies impaired the PD-1-elevating activity of CLL cell supernatants in healthy CTLs. These data were confirmed using recombinant IL-9 that, as opposed to recombinant IL-10, enhanced surface PD-1 expression in

healthy CTLs cultured in healthy B cell-conditioned media (**Fig. 13A, 13B**). These data indicate that IL-9, but not IL-10, mediates the PD-1-elevating ability of leukemic cells on healthy CTLs.

We correlated PD-1 expression on $CD8^+$ cells with IL-9 expression in CLL cells. PD-1 expression on $CD8^+$ cells directly correlated with IL-9 expression in patient-matched leukemic cells. The heat map shown in **figure 13C**, which correlates PD-1 expression in $CD8^+$ cells with both IL-9 and p66Shc expression in patient matched leukemic cells, highlighted a strong correlation among the three markers, with PD-1 expression on $CD8^+$ cells directly correlated with IL-9 but inversely correlated with p66Shc expression in leukemic cells (**Fig. 13C**). These results highlight a new mechanism exploited by CLL cells to disable the tumor-suppressive activity of CTLs involving IL-9 secretion into the TME to enhance PD-1 expression in CTLs.

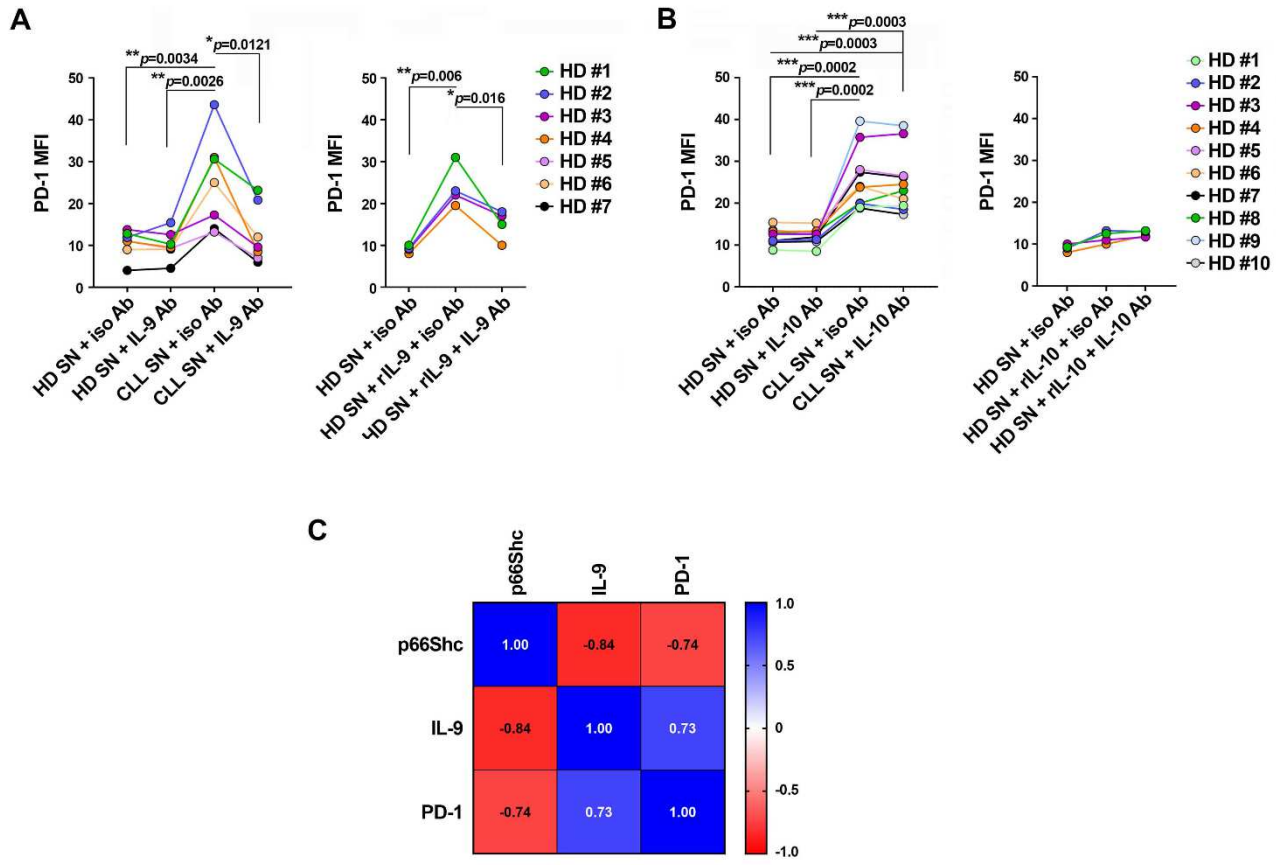

Figure 13. IL-9 secreted by CLL cells promotes PD-1 expression in CTLs. A, B. Flow cytometric analysis of surface PD-1 in $CD8^+$ cells purified from buffy coats, stimulated with anti-CD3/CD28 mAb-coated beads + IL-2 for 48 h (CTLs), and cultured in conditioned media in the presence of either control (iso Ab), anti-IL-860 9 (IL-9 Ab, **A**) or anti-IL-10 (IL-10 Ab, **B**) antibodies and/or recombinant IL-9 (rIL-9) (**A**), or recombinant IL-10 (rIL-10) (**B**) (n buffy coats from healthy donors = 4). **C**. Spearman r correlation index between surface PD-1 (MFI) in $CD8^+$ cells isolated from CLL patients and IL-9 and p66Shc mRNA in CLL cells from the respective CLL patients (n=18). Data are expressed as mean±SD (A, B); one-way ANOVA test (A, B); Sperman r correlation index (C). ****, $p \leq 0.0001$; ***, $p \leq 0.001$; **, $p \leq 0.01$; *, $p \leq 0.05$.

3.6 IL-9 secreted by leukemic cells from CLL patients impairs IS formation in CTLs

CLL cells suppress the ability of activated $CD8^+$ cells to assemble the IS through direct interaction of surface inhibitory receptor/ligand axes (**Fig. 9L**).[91] To test the hypothesis that CLL cell-derived IL-9 contributes to the assembly of dysfunctional ISs by modulating PD-1 expression in CTLs, healthy $CD8^+$ cells were cultured with healthy B cell or CLL cell-conditioned media in the presence of either isotype control or anti-IL-9 neutralizing antibodies prior to conjugate formation. Anti-IL-9 antibodies counteracted the suppressive activities of leukemic cell supernatants on IS formation (**Fig. 14A - 14D**, *left panels*). Consistent with these findings, recombinant IL-9 added to healthy B cell conditioned media impaired IS formation, an effect that was not observed in the presence of neutralizing anti-IL-9 antibodies (**Fig. 14A - 14D**). Consistent with the IS defects (**Fig. 14A - 14D**), the suppressive activity of the CLL supernatants on CTL-mediated killing and degranulation were neutralized by anti-IL-9 antibodies (**Fig. 14E, 14F**). Moreover, recombinant IL-9 reproduced the suppressive activities of CLL supernatants (**Fig. 14E, 14F**). Collectively, these results demonstrate that CLL cell-derived IL-9 impairs IS formation and effector functions of CTLs by promoting PD-1 expression in CTLs.

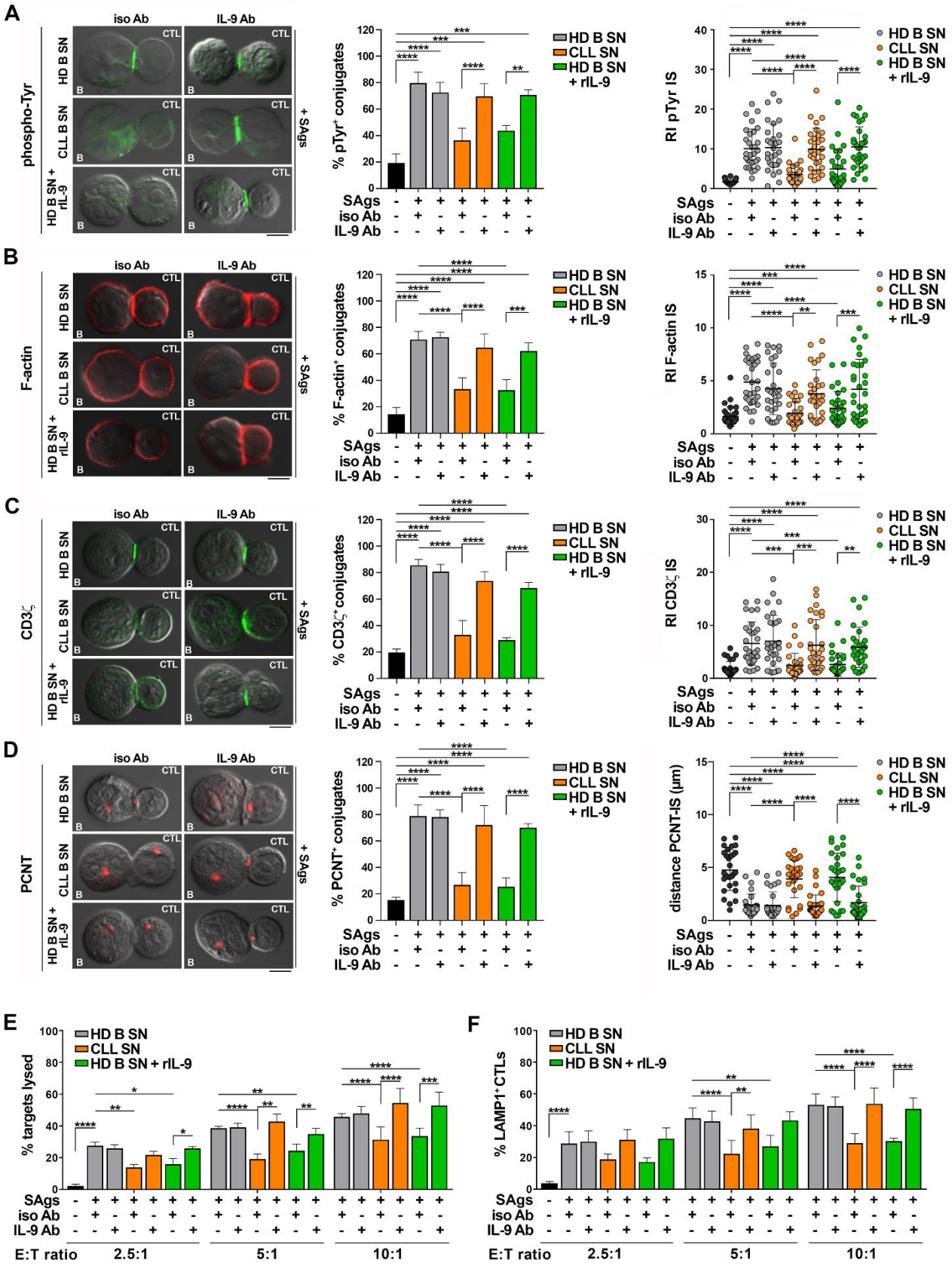
A
B
C
D
E
F
iso Ab
IL-9 Ab
CTL
HD B SN
CLL B SN
HD B SN + rIL-9
+ SAgs
phospho-Tyr
F-actin
CD3ζ
PCNT
% pTyr+ conjugates
% F-actin+ conjugates
% CD3ζ+ conjugates
% PCNT+ conjugates
RI pTyr IS
RI F-actin IS
RI CD3ζ IS
distance PCNT-IS (µm)
% targets lysed
% LAMP1+ CTLs
HD B SN
CLL SN
HD B SN + rIL-9
SAgs
iso Ab
IL-9 Ab
E:T ratio
2.5:1
5:1
10:1

Figure 14. IL-9 secreted by CLL cells suppresses IS formation and effector functions in CTLs. A-D, *left panels.* Immunofluorescence analysis of pTyr (**A**), F-actin (**B**), CD3ζ (**C**), and PCNT (**D**) in CTLs activated for 48 h in the presence of conditioned media, with the addition of either control (iso Ab), anti-IL-9 (IL-9 Ab) or recombinant IL-9 (rIL-9), mixed with Raji cells (APCs) either unpulsed or pulsed with a combination of SAgs, and incubated for 15 min at 37°C. Data are expressed as % of 15 min SAg-specific conjugates harboring staining at the IS (≥50 cells/sample, n independent experiments ≥3). Representative images (medial optical sections) of the T cell:APC conjugates are shown. Scale bar, 5 μm. **A-C**, *right panels.* Relative fluorescence intensity of pTyr (**A**), F-actin (**B**), and CD3ζ (**C**) at the IS (recruitment index, RI; 10 cells/sample, n independent experiments ≥3. **D**, *right panel*. Measurement of the distance (μm) of the centrosome (PCNT) from the CTL:APC contact in conjugates formed as above (10 cells/sample, n independent experiments =3). ***E***. Flow cytometric analysis of target cell killing by CTLs cultured for 7 days in conditioned media, with the addition of either control (iso Ab), anti-IL-9 (IL-9 Ab) or recombinant IL-9 (rIL-9), using SAg-loaded Raji cells as targets at an E:T cell ratio 2.5:1, 5:1 and 10:1. Cells were cocultured for 4 h and stained with propidium iodide prior to processing for flow cytometry. Analyses were carried out gating on $CFSE^+PI^+$ cells. The histogram shows the percentage (%) of target cells lysed (n independent experiments =5). **F**. Flow cytometric analysis of degranulation of CTLs cultured for 7 days as in (**E**), then cocultured with CFSE-stained Raji cells loaded with SAg at an E:T cell ratio 2.5:1, 5:1 and 10:1 for 4 h. The histogram shows the percentage (%) of $LAMP1^+$ CTLs, measured gating on the CSFE-negative population (n=6). Data are expressed as mean±SD (A-F): one-way ANOVA test (A-D); two-way ANOVA test (E, F). ****, $p \leq 0.0001$; ***, $p \leq 0.001$; **, $p \leq 0.01$; *, $p \leq 0.05$.

3.7 In vivo IL-9 blockade in Eμ-TCL1/p66$^{-/-}$ mice normalizes PD-1 expression in CD8$^+$ cells

To validate the role of IL-9 in PD-1 overexpression in $CD8^+$ cells in vivo, we carried out IL-9-blockade experiments in the aggressive CLL Eμ-TCL1/p66Shc$^{-/-}$ mouse model.[104,49] Mice with overt disease were intraperitoneally administered anti-IL-9 or isotype-control mAbs twice a week for 4 weeks (**Fig. 15A**).[49] Flow cytometry analysis of PD-1^+CD8^+ splenocytes demonstrated that IL-9 blockade resulted in a reduction in PD1 expression and frequency of PD-1^+CD8^+ cells compared to isotype control (**Fig. 15B**). Hence, in the presence of anti-IL9 antibodies neutralized the enhancement in PD-1 expression induced by Eμ-TCL1/p66Shc$^{-/-}$ leukemic cell, indicating that IL-9 shape the microenvironment to pro-tumoral one.

8. Ex vivo and in vivo inhibition of BTK enhances IL-9 expression in leukemic cells from CLL patients

Treatment of CLL patients with BTK inhibitors relieves T cell exhaustion by downregulating PD-1 expression.[84,120] We hypothesized that this could partly or completely account for the enhanced release of IL-9 in the TME by leukemic cells. To test this hypothesis, IL-9 secreted in media conditioned by CLL cells treated in vitro for 48 h with the BTK inhibitor Ibrutinib was quantified by ELISA. Ibrutinib treatment decreased IL-9 release by CLL cells (**Fig. 15C**). Moreover, IL-9 expression was reduced in 4 CLL patients showing a significant response to second line Ibrutinib treatment (range follow-up 26.2±7.3 months) (**Fig. 15E, Table 4**), suggesting that the response of

CLL patients to BTK inhibitors results, at least in part, from the normalization of IL-9 release by leukemic cells.

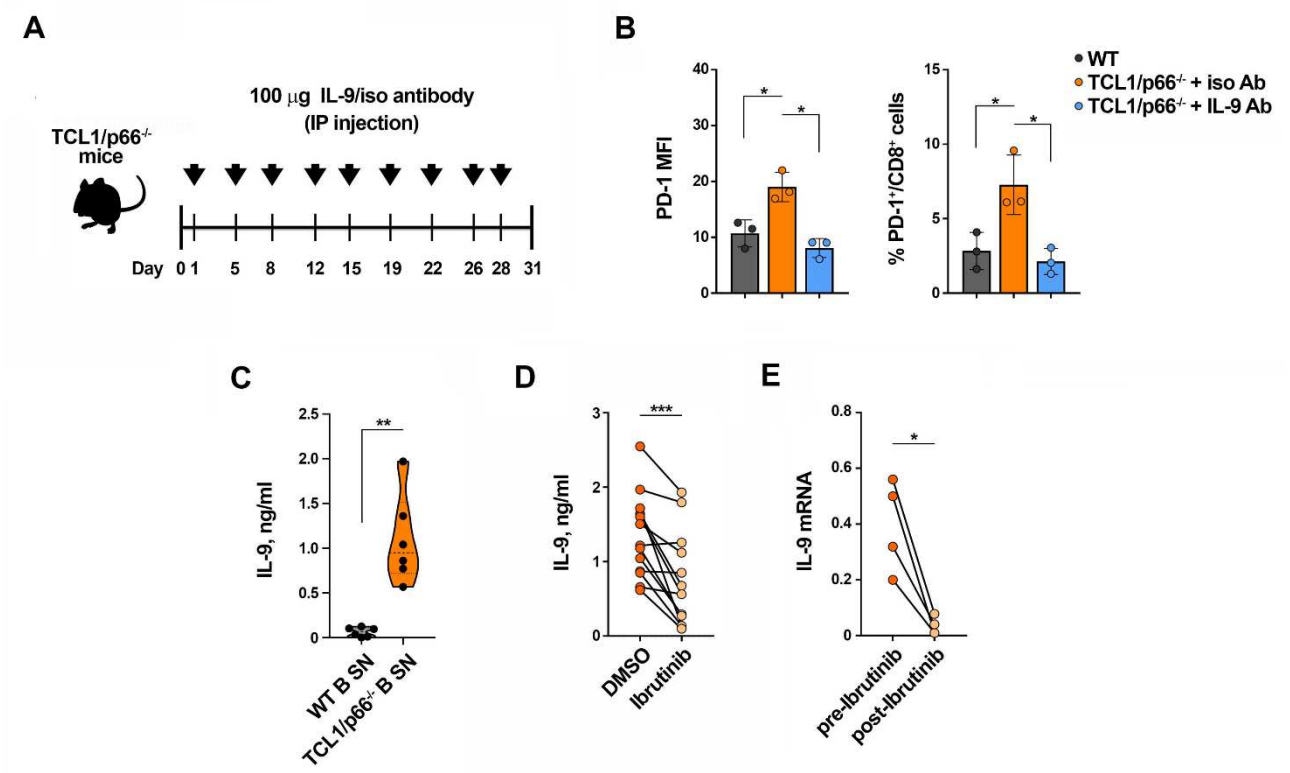

Figure 15. In vivo IL-9 blockade in Eμ-TCL1/p66$^{-/-}$ mice normalizes PD-1 expression in CD8^{+} cells. **A.** Schematic representation of the experimental design of intraperitoneal injection of wild-type C57BL/6 mice (n=3) or Eμ-TCL1/p66Shc$^{-/-}$ mice (n=6) with overt leukemia (~40% CD5^{+}CD19^{+} leukemic cells in PB) with 100 μg of either isotype control (n=3) or anti-IL-9 (n=3) antibodies dissolved in 100 μl PBS. **B**. Flow cytometric analysis of PD-1^{+}CD8^{+} cells in spleens isolated from either wild type mice injected with PBS (n=3) or Eμ-TCL1/p66Shc$^{-/-}$ mice (n=6) injected with anti-IL-9 (IL-9 Ab, n=3) or isotype (iso Ab, n=3) mAb. Data are expressed as MFI of PD-1 in CD8^{+}-gated cells (left) and as % PD-1^{+}CD8^{+} cells (right). **C**. Quantification by ELISA of IL-9 released in the culture supernatants of leukemic cells isolated from peripheral blood of CLL patients (n=13) and treated in vitro for 48 h with either DMSO or 10 μM Ibrutinib. **D**. qRT-PCR analysis of mRNA expression of IL-9 in leukemic cells isolated from peripheral blood of CLL patients (n=4) who received 420 mg Ibrutinib once a day. Blood samples were collected on the starting day of Ibrutinib treatment (before Ibrutinib) and at follow-up of Ibrutinib treatment (follow-up Ibrutinib; range follow-up 26.2±7.3 months). Data are expressed as mean±SD (B): RM one-way ANOVA (B); Paired t test (C, D). ****, $p \leq 0.0001$; **, $p \leq 0.01$; *, $p \leq 0.05$.

Part II

DISCUSSION

Tumor cells develop mechanisms to escape immune surveillance. CTLs are subjected to these suppressive actions, as demonstrated by impairment in their anti-tumoral functions.[112] Direct inhibitory receptor/ligand axes contribute to CTL suppression by inhibiting TCR-dependent signaling pathways.[112] Here we identify a new cell contact-independent mechanism of CLL cell escape from CTL-mediated killing.

Within the TME, CLL cells secrete cytokines and chemokines in order to sustain and favour a pro-tumorigenic loop,[121–123] as exemplified by Interleukin (IL)-10, that suppress the ability of monocytes/macrophages to produce TNF-α.[124] Of note, CLL cells also secrete cytokines with well-known anti-tumoral activities[122], such as IL-15 which enhances antibody-dependent cytotoxicity against CLL cells in *vitro*.[125] Moreover, low IL-27 serum levels in CLL patients have been associated with the onset of aggressive disease and a decrease in the anti-leukemic cytotoxicity of $CD8^+$ cells.[126] Conversely, elevated levels of IL-6 in the serum of CLL patients are correlated with a suppressed functional profile of circulating CTLs.[127,128] Notably, the direct involvement of IL-6 in CTL suppression in CLL has yet to be assessed.

Abnormal IL9 secretion by leukemic cells is observed in CLL patients.[71,49,129,130] In the CLL mouse model Eμ-TCL1, IL-9 abnormal secretion correlates with aggressive disease hallmarks, such as unmutated *IGHV*, low p66Shc levels [49,123], and lower overall survival [49].The pro-tumoral activity of IL-9 involves its ability to stimulate stromal cells to secrete homing chemokines, which in turn contribute to attract CLL cells to the pro-survival lymphoid niche.[49,123,124] Moreover, IL9 blockade in Eμ-TCL1 mice decreases leukemic cell invasiveness and disease burden,[49,123,124] suggesting a role of IL-9 in CLL pathogenesis.

Here, we found that IL-9 is a key pro-tumoral cytokine that shapes the TME not only to promote leukemic cell accumulation and survival,[49] but also to help them evade from CTL killing by enhancing PD-1 expression.

PD-1 is a known inhibitory receptor expressed on several cell types, such as effector T cells, but it is almost absent in resting T cells.[112,131,132] Several stimuli upregulate PD-1 expression, the most important being TCR-mediated signaling, which activates transcription factors implicated in PD-1 expression, including nuclear factor of activated T cells 1 (NFATC1)[133,134], NF-κB[131], and T-bet[134]. Cytokines such as IL-10[132] and TGF-β[132,135] have been also found to promote PD-1 expression. Here, we show that IL-9 secreted by leukemic cells from CLL patients with aggressive disease

presentation enhances PD-1 expression in healthy CTLs, thereby contributing to shift them to the exhausted and disabled phenotype. The results suggest that agents targeting IL-9, such as IL-9 neutralising antibodies, could be used in combination with immune checkpoint inhibitor therapies to reverse the state of exhaustion and promote immune responses against tumor cells in CLL patients.

In support of this notion, suppression of IL-10 expression has been shown to enhance anti-tumor T cell immunity in combination with PD-L1 blockade in a preclinical mouse model[136]. However, IL-10 suppression alone in vivo increased the frequency of $CD8^+$ cells showing effector markers, but it did not affect PD-1 upregulation[136], consistent with our findings.

Although CLL patients exhibit an accumulation of $PD1^+CD8^+$ cells in peripheral lymphoid organs, PD-1/PD-L1 inhibitory signaling axis blockade alone has shown limited clinical efficacy, with the exception of the most aggressive development of the disease, Richter's transformation.[100] Consequently, the neutralization of PD-1/PD-L1 axis may be insufficient to reactivate the anti-tumor functions of CTLs, highlighting the crucial role of inhibitory molecules beyond PD-1, such as CTLA-4 and LAG-3,[2,137,138] in limiting CTL functions.

Our results showing a recovery of the ability of exhausted CTLs to form functional IS in the presence of neutralizing anti-PD-1 antibodies underscore the crucial role of PD-1 in the suppression of anti-tumor CTL activities in the complex context of TME. Indeed, expression of both CTLA-4 and LAG-3 was not altered by CLL cell-conditioned media, ruling them out as mediators of CTL exhaustion mediated by soluble factors in CLL.

Additionally, our data show that the ability of CLL cells to suppress CTLs also depends on the defective expression of p66Shc, a molecular adaptor that promotes apoptosis through an adaptor-independent pro-oxidant activity,[96,98] suggesting a key role of this adaptor in promoting the formation of a pro-survival TME for leukemic cells. Reduced p66Shc expression promotes CLL cell survival by altering intrinsic apoptosis mechanisms, and contributes to leukemic cell chemoresistance.[104,49,139] Furthermore, p66Shc activity, which modulates gene expression by elevating intracellular ROS levels , promotes CLL cell survival by altering the balance between homing and egress receptors that coordinate lymphocyte trafficking. This promotes the accumulation of leukemic cells in pro-survival lymphoid niches.[140,141] Here we show that reduced expression of p66Shc in Eμ-TCL1 mice is also involved in the expression of CLL-critical cytokines such as IL-9 and IL-10 by leukemic cells. This condition is also found in p66Shc-deficient CLL cells. These results highlight how the p66Shc defect in CLL cells is involved in processes that are crucial for the tumor cell survival.

The data obtained from this work underline how CLL cells engage a crosstalk with CTLs in the TME in order to evade immunosurveillance. By implementing a cell contact-independent

mechanism, CLL cells are able to inhibit the killing capacity of CTLs by releasing soluble factors such as IL-9. Leukemic cell-derived IL-9 in turn induces an increased expression of exhaustion markers and alters the formation of a functional IS, thereby favouring the survival of leukemic cells and contributing to the pathogenesis of CLL.

BIBLIOGRAPHY

1. Thomas J. Kipps1, Freda K. Stevenson2, Catherine J. Wu3, Carlo M. Croce4, Graham Packham2, William G. Wierda5, Susan O'Brien6, John Gribben7, and K. R. Chronic lymphocytic leukaemia. *Med. (United Kingdom)* **49**, 286–292 (2017).
2. Hallek, M. *et al.* iwCLL guidelines for diagnosis, indications for treatment, response assessment, and supportive management of CLL. *Blood* **131**, 2745–2760 (2018).
3. Landgren, O., Gridley, G., Check, D., Caporaso, N. E. & Morris Brown, L. Acquired immune-related and inflammatory conditions and subsequent chronic lymphocytic leukaemia. *Br. J. Haematol.* **139**, 791–798 (2007).
4. Wiernik, P. H., Ashwin, M., Hu, X. P., Paietta, E. & Brown, K. Anticipation in familial chronic lymphocytic leukaemia. *Br. J. Haematol.* **113**, 407–414 (2001).
5. Scarfò, L., Ferreri, A. J. M. & Ghia, P. Chronic lymphocytic leukaemia. *Crit. Rev. Oncol. Hematol.* **104**, 169–182 (2016).
6. ten Hacken, E. & Burger, J. A. Microenvironment interactions and B-cell receptor signaling in Chronic Lymphocytic Leukemia: Implications for disease pathogenesis and treatment. *Biochim. Biophys. Acta - Mol. Cell Res.* **1863**, 401–413 (2016).
7. Scarfò, L., Ferreri, A. J. M. & Ghia, P. Chronic lymphocytic leukaemia. *Crit. Rev. Oncol. Hematol.* **104**, 169–182 (2016).
8. Packham, G. & Stevenson, F. K. Bodyguards and assassins: Bcl-2 family proteins and apoptosis control in chronic lymphocytic leukaemia. *Immunology* **114**, 441–449 (2005).
9. Ghia, P. & Caligaris-Cappio, F. The indispensable role of microenvironment in the natural history of low-grade B-cell neoplasms. *Adv. Cancer Res.* **79**, 157–173 (2000).
10. Ashkenazi, A. & Salvesen, G. Regulated cell death: signaling and mechanisms. *Annu. Rev. Cell Dev. Biol.* **30**, 337–356 (2014).
11. Billard, C. Apoptosis inducers in chronic lymphocytic leukemia. *Oncotarget* **5**, 309–325 (2014).
12. Cimmino, A. *et al.* miR-15 and miR-16 induce apoptosis by targeting BCL2. *Proc. Natl. Acad. Sci. U. S. A.* **102**, 13944–13949 (2005).
13. Pedersen, I. M. & Reed, J. C. Microenvironmental interactions and survival of CLL B-cells. *Leuk. Lymphoma* **45**, 2365–2372 (2004).
14. Burger, J. A. Nurture versus nature: the microenvironment in chronic lymphocytic leukemia. *Hematology Am. Soc. Hematol. Educ. Program* **2011**, 96–103 (2011).
15. Willimott, S. & Wagner, S. D. miR-125b and miR-155 contribute to BCL2 repression and

proliferation in response to CD40 ligand (CD154) in human leukemic B-cells. *J. Biol. Chem.* **287**, 2608–2617 (2012).

16. Kurtova, A. V. *et al.* Diverse marrow stromal cells protect CLL cells from spontaneous and drug-induced apoptosis: Development of a reliable and reproducible system to assess stromal cell adhesion-mediated drug resistance. *Blood* **114**, 4441–4450 (2009).
17. Ghia, P. *et al.* Chronic lymphocytic leukemia B cells are endowed with the capacity to attract CD4+,CD40L+ T cells by producing CCL22. *Eur. J. Immunol.* **32**, 1403–1413 (2002).
18. Nicholas, N. S., Apollonio, B. & Ramsay, A. G. Tumor microenvironment (TME)-driven immune suppression in B cell malignancy. *Biochim. Biophys. Acta - Mol. Cell Res.* **1863**, 471–482 (2016).
19. Vardi, A. *et al.* Restrictions in the T-cell repertoire of chronic lymphocytic leukemia: High-throughput immunoprofiling supports selection by shared antigenic elements. *Leukemia* **31**, 1555–1561 (2017).
20. Nunes, C. *et al.* Expansion of a CD8 +PD-1 + replicative senescence phenotype in early stage CLL patients is associated with inverted CD4:CD8 ratios and disease progression. *Clin. Cancer Res.* **18**, 678–687 (2012).
21. Riches, J. C. *et al.* T cells from CLLpatients exhibit features of T-cell exhaustion but retain capacity for cytokine production. *Blood* **121**, 1612–1621 (2013).
22. Kabanova, A. *et al.* Human Cytotoxic T Lymphocytes Form Dysfunctional Immune Synapses with B Cells Characterized by Non-Polarized Lytic Granule Release. *Cell Rep.* **15**, 9–18 (2016).
23. Kabanova, A., Zurli, V. & Baldari, C. T. Signals controlling lytic granule polarization at the cytotoxic immune synapse. *Front. Immunol.* **9**, 1–13 (2018).
24. Corda, D., Zizza, P., Varone, A., Filippi, B. M. & Mariggiò, S. The glycerophosphoinositols: Cellular metabolism and biological functions. *Cell. Mol. Life Sci.* **66**, 3449–3467 (2009).
25. Mariggio, S. *et al.* A novel pathway of cell growth regulation mediated by a PLA 2 α-derived phosphoinositide metabolite . *FASEB J.* **20**, 2567–2569 (2006).
26. Patrussi, L., Mariggiò, S., Corda, D. & Baldari, C. T. The glycerophosphoinositols: From lipid metabolites to modulators of T-cell signaling. *Front. Immunol.* **4**, 1–6 (2013).
27. Berrie, C. P. *et al.* Maintenance of PtdIns45P2 pools under limiting inositol conditions, as assessed by liquid chromatography-tandem mass spectrometry and PtdIns45P2 mass evaluation in Ras-transformed cells. *Eur. J. Cancer* **38**, 2463–2475 (2002).
28. Corda, D., Iurisci, C. & Berrie, C. P. Biological activities and metabolism of the lysophosphoinositides and glycerophosphoinositols. *Biochim. Biophys. Acta - Mol. Cell Biol.*

Lipids **1582**, 52–69 (2002).

29. Berrie, C. P., Iurisci, C., Piccolo, E., Bagnati, R. & Corda, D. Analysis of Phosphoinositides and Their Aqueous Metabolites. *Methods Enzymol.* **434**, 187–232 (2007).
30. French, P. J. *et al.* Changes in the levels of inositol lipids and phosphates during the differentiation of HL60 promyelocytic cells towards neutrophils or monocytes. *Proc. R. Soc. B Biol. Sci.* **245**, 193–201 (1991).
31. Bunce CM, French PJ, Pat- ton WN, Turnell AS, Scott SA, Michell RH, et al. Levels of inositol m etabolites w ithin norm al myeloid blast cells and changes during their differentiation towards monocytes. *Proc Biol Sci* 27–33 (1992).
32. Mountford, J. C., Bunce, C. M., French, P. J., Michell, R. H. & Brown, G. Intracellular concentrations of inositol, glycerophosphoinositol and inositol pentakisphosphate increase during haemopoietic cell differentiation. *BBA - Mol. Cell Res.* **1222**, 101–108 (1994).
33. Patrussi, L. *et al.* Glycerophosphoinositol-4-phosphate enhances SDF-1α-stimulated T-cell chemotaxis through PTK-dependent activation of Vav. *Cell. Signal.* **19**, 2351–2360 (2007).
34. Vessichelli, M. *et al.* The natural phosphoinositide derivative glycerophosphoinositol inhibits the lipopolysaccharide-induced inflammatory and thrombotic responses. *J. Biol. Chem.* **292**, 12828–12841 (2017).
35. Zhang, J., Somani, A. K. & Siminovitch, K. A. Roles of the SHP-1 tyrosine phosphatase in the negative regulation of cell signalling. *Semin. Immunol.* **12**, 361–378 (2000).
36. Yang, J. *et al.* Crystal structure of human protein-tyrosine phosphatase SHP-1. *J. Biol. Chem.* **278**, 6516–6520 (2003).
37. Varone, A. *et al.* A signalling cascade involving receptor-activated phospholipase A2, glycerophosphoinositol 4-phosphate, Shp1 and Src in the activation of cell motility. *Cell Commun. Signal.* **17**, 1–21 (2019).
38. Varone, A., Spano, D. & Corda, D. Shp1 in Solid Cancers and Their Therapy. *Front. Oncol.* **10**, 1–10 (2020).
39. Chai, H., Luo, A. Z., Weerasinghe, P. & Brown, R. E. Sorafenib downregulates ERK/Akt and STAT3 survival pathways and induces apoptosis in a human neuroblastoma cell line. *Int. J. Clin. Exp. Pathol.* **3**, 408–415 (2010).
40. Zhang, H. *et al.* Anticancer activity of dietary xanthone α-mangostin against hepatocellular carcinoma by inhibition of STAT3 signaling via stabilization of SHP1. *Cell Death Dis.* **11**, (2020).
41. Saraswati, S., Alhaider, A., Abdelgadir, A. M., Tanwer, P. & Korashy, H. M. Phloretin attenuates STAT-3 activity and overcomes sorafenib resistance targeting SHP-1-mediated

inhibition of STAT3 and Akt/VEGFR2 pathway in hepatocellular carcinoma. *Cell Commun. Signal.* **17**, 1–18 (2019).

42. Gan, L. *et al.* Epigallocatechin-3-gallate induces apoptosis in acute promyelocytic leukemia cells via a SHP-1-p38α MAPK-bax cascade. *Oncol. Lett.* **14**, 6314–6320 (2017).
43. Tibaldi, E. *et al.* Targeted activation of the SHP-1/PP2A signaling axis elicits apoptosis of chronic lymphocytic leukemia cells. *Haematologica* **102**, 1401–1412 (2017).
44. Tibaldi, E. *et al.* Lyn-mediated SHP-1 recruitment to CD5 contributes to resistance to apoptosis of B-cell chronic lymphocytic leukemia cells. *Leukemia* **25**, 1768–1781 (2011).
45. Campos, A. M. *et al.* Direct LC-MS/MS Analysis of Extra- and Intracellular Glycerophosphoinositol in Model Cancer Cell Lines. *Front. Immunol.* **12**, 1–8 (2021).
46. Varone, A. *et al.* The phosphatase Shp1 interacts with and dephosphorylates cortactin to inhibit invadopodia function. *Cell Commun. Signal.* **19**, 1–22 (2021).
47. Visentin, A. *et al.* Prognostic and Predictive Effect of IGHV Mutational Status and Load in Chronic Lymphocytic Leukemia: Focus on FCR and BR Treatments. *Clin. Lymphoma, Myeloma Leuk.* **19**, 678-685.e4 (2019).
48. Marani, M., Tenev, T., Hancock, D., Downward, J. & Lemoine, N. R. Identification of Novel Isoforms of the BH3 Domain Protein Bim Which Directly Activate Bax To Trigger Apoptosis. *Mol. Cell. Biol.* **22**, 3577–3589 (2002).
49. Patrussi, L. *et al.* Enhanced IL-9 secretion by p66Shc-deficient CLL cells modulates the chemokine landscape of the stromal microenvironment. *Blood* **137**, 2182–2195 (2021).
50. Xiao, W., Ando, T., Wang, H. Y., Kawakami, Y. & Kawakami, T. Lyn-and PLC-β3-dependent regulation of SHP-1 phosphorylation controls Stat5 activity and myelomonocytic leukemia-like disease. *Blood* **116**, 6003–6013 (2010).
51. Bellosillo, B. *et al.* Spontaneous and drug-induced apoptosis is mediated by conformational changes of Bax and Bak in B-cell chronic lymphocytic leukemia. *Blood* **100**, 1810–1816 (2002).
52. Roberts, A. W. *et al.* Targeting BCL2 with Venetoclax in Relapsed Chronic Lymphocytic Leukemia. *N. Engl. J. Med.* **374**, 311–322 (2016).
53. Mohamed Rahmani1, 2, Jewel Nkwocha1, Elisa Hawkins1, Xinyan Pei1, R. E. P. & Maciej Kmieciak1, Joel D. Leverson7, Deepak Sampath8, Andrea Ferreira-Gonzalez6, and S. G. Co-targeting BCL-2 and PI3K induces BAX-dependent mitochondrial apoptosis in AML cells Mohamed. *Physiol. Behav.* **176**, 139–148 (2017).
54. A., C. B. & El-Deiry, W. S. Targeting apoptosis in cancer therapy. *Physiol. Behav.* **176**, 139–148 (2016).

55. Hallek, M. Chronic lymphocytic leukemia: 2020 update on diagnosis, risk stratification and treatment. *Am. J. Hematol.* **94**, 1266–1287 (2019).
56. Cervantes-Gomez, F. *et al.* Pharmacological and protein profiling suggests venetoclax (ABT-199) as optimal partner with ibrutinib in chronic lymphocytic leukemia. *Clin. Cancer Res.* **21**, 3705–3715 (2015).
57. Thijssen, R. *et al.* Resistance to ABT-199 induced by microenvironmental signals in chronic lymphocytic leukemia can be counteracted by CD20 antibodies or kinase inhibitors. *Haematologica* **100**, (2015).
58. Zhiqing Liu, Ye Ding, Na Ye, ChristopherWild, Haiying Chen, and J. Z. & Chemical. Direct Activation of Bax Protein for Cancer Therapy. *Harv. Bus. Rev.* **86**, 84–92 (2008).
59. Zhou, Z. *et al.* Entinostat combined with Fludarabine synergistically enhances the induction of apoptosis in TP53 mutated CLL cells via the HDAC1/HO-1 pathway. *Life Sci.* **232**, 116583 (2019).
60. Rahmani, M. *et al.* Cotargeting BCL-2 and PI3K induces BAX-dependent mitochondrial apoptosis in AML cells. *Cancer Res.* **78**, 3075–3086 (2018).
61. Fürstenau, M. & Eichhorst, B. Novel agents in chronic lymphocytic leukemia: New combination therapies and strategies to overcome resistance. *Cancers (Basel).* **13**, 1–18 (2021).
62. Stornaiuolo, M. *et al.* Structure-based lead optimization and biological evaluation of BAX direct activators as novel potential anticancer agents. *J. Med. Chem.* **58**, 2135–2148 (2015).
63. Zhao, G. *et al.* Activation of the Proapoptotic Bcl-2 Protein Bax by a Small Molecule Induces Tumor Cell Apoptosis. *Mol. Cell. Biol.* **34**, 1198–1207 (2014).
64. Xin, M. *et al.* Small-molecule Bax agonists for cancer therapy. *Nat. Commun.* **5**, (2014).
65. Liu, G. *et al.* Structure-activity relationship studies on Bax activator SMBA1 for the treatment of ER-positive and triple-negative breast cancer. *Eur. J. Med. Chem.* **178**, 589–605 (2019).
66. Vervloessem, T. *et al.* BDA-366, a putative Bcl-2 BH4 domain antagonist, induces apoptosis independently of Bcl-2 in a variety of cancer cell models. *Cell Death Dis.* **11**, (2020).
67. Zhang, S. & Kipps, T. J. The pathogenesis of chronic lymphocytic leukemia. *Annu. Rev. Pathol. Mech. Dis.* **9**, 103–118 (2014).
68. Stevenson, F. K., Forconi, F. & Packham, G. The Meaning and Relevance of B-Cell Receptor Structure and Function in Chronic Lymphocytic Leukemia. *Semin. Hematol.* **51**, 158–167 (2014).
69. Zou, Z. J. *et al.* miR-26a and miR-214 down-regulate expression of the PTEN gene in

chronic lymphocytic leukemia, but not PTEN mutation or promoter methylation. *Oncotarget* **6**, 1276–1285 (2015).

70. Zonta, F. *et al.* Lyn sustains oncogenic signaling in chronic lymphocytic leukemia by strengthening SET-mediated inhibition of PP2A. *Blood* **125**, 3747–3755 (2015).
71. Cui, B. *et al.* Micro RNA-155 influences B-cell receptor signaling and associates with aggressive disease in chronic lymphocytic leukemia. *Blood* **124**, 546–554 (2014).
72. Tsui, F. W. L., Martin, A., Wang, J. & Tsui, H. W. Investigations into the regulation and function of the SH2 domain-containing protein-tyrosine phosphatase, SHP-1. *Immunol. Res.* **35**, 127–136 (2006).
73. Dempke, W. C. M., Uciechowski, P., Fenchel, K. & Chevassut, T. Targeting SHP-1, 2 and SHIP Pathways: A novel strategy for cancer treatment? *Oncol.* **95**, 257–269 (2018).
74. Chen, H. *et al.* Allicin Inhibits Proliferation and Invasion in Vitro and in Vivo via SHP-1-Mediated STAT3 Signaling in Cholangiocarcinoma. *Cell. Physiol. Biochem.* **47**, 641–653 (2018).
75. Pardoll, D. M. The blockade of immune checkpoints in cancer immunotherapy. *Nat Rev Cancer* 252–264 (2012) doi:10.1103/PhysRevB.97.115128.
76. Greaves, P. & Gribben, J. G. The role of B7 family molecules in hematologic malignancy. *Blood* **121**, 734–744 (2013).
77. Freeman, G. J. *et al.* Engagement of the PD-1 immunoinhibitory receptor by a novel B7 family member leads to negative regulation of lymphocyte activation. *J. Exp. Med.* **192**, 1027–1034 (2000).
78. Xiao, Y. *et al.* RGMb is a novel binding partner for PD-l2 and its engagement with PD-l2 promotes respiratory tolerance. *J. Exp. Med.* **211**, 943–959 (2014).
79. Sharpe, A. H. & Pauken, K. E. The diverse functions of the PD1 inhibitory pathway. *Nat. Rev. Immunol.* **18**, 153–167 (2018).
80. Marasco, M. *et al.* Molecular mechanism of SHP2 activation by PD-1 stimulation. *Sci. Adv.* **6**, (2020).
81. Mahoney, K. M., Rennert, P. D. & Freeman, G. J. Combination cancer immunotherapy and new immunomodulatory targets. *Nat. Rev. Drug Discov.* **14**, 561–584 (2015).
82. Brusa, D. *et al.* The PD-1/PD-L1 axis contributes to T-cell dysfunction in chronic lymphocytic leukemia. *Haematologica* **98**, 953–963 (2013).
83. Wherry, E. J. T cell exhaustion. *Nat. Immunol.* **12**, 492–499 (2011).
84. Long, M. *et al.* Ibrutinib treatment improves T cell number and function in CLL patients. *J. Clin. Invest.* **127**, 3052–3064 (2017).

85. Dustin, M. L. & Choudhuri, K. Signaling and Polarized Communication Across the T Cell Immunological Synapse. *Annu. Rev. Cell Dev. Biol.* **32**, 303–325 (2016).
86. Huse, M. Microtubule-organizing center polarity and the immunological synapse: Protein kinase C and beyond. *Front. Immunol.* **3**, 1–11 (2012).
87. Ritter, A. T. *et al.* Actin Depletion Initiates Events Leading to Granule Secretion at the Immunological Synapse. *Immunity* **42**, 864–876 (2015).
88. Lettau, M., Kabelitz, D. & Janssen, O. Lysosome-Related Effector Vesicles in T Lymphocytes and NK Cells. *Scand. J. Immunol.* **82**, 235–243 (2015).
89. Stinchcombe, J. C., Majorovits, E., Bossi, G., Fuller, S. & Griffiths, G. M. Centrosome polarization delivers secretory granules to the immunological synapse. *Nature* **443**, 462–465 (2006).
90. Burger, J. A. & Gribben, J. G. The microenvironment in chronic lymphocytic leukemia (CLL) and other B cell malignancies: Insight into disease biology and new targeted therapies. *Semin. Cancer Biol.* **24**, 71–81 (2014).
91. Ramsay, A. G., Clear, A. J., Fatah, R. & Gribben, J. G. Multiple inhibitory ligands induce impaired T-cell immunologic synapse function in chronic lymphocytic leukemia that can be blocked with lenalidomide: Establishing a reversible immune evasion mechanism in human cancer. *Blood* **120**, 1412–1421 (2012).
92. Ramsay, A. G. *et al.* Chronic lymphocytic leukemia T cells show impaired immunological synapse formation that can be reversed with an immunomodulating drug. *J. Clin. Invest.* **118**, 2427–2437 (2008).
93. Nakamura, T., Muraoka, S., Sanokawa, R. & Mori, N. N-Shc and Sck, two neuronally expressed Shc adapter homologs. Their differential regional expression in the brain and roles in neurotrophin and Src signaling. *J. Biol. Chem.* **273**, 6960–6967 (1998).
94. Cattaneo, E. & Pelicci, P. G. Emerging roles for SH2/PTB-containing Shc adaptor proteins in the developing mammalian brain. *Trends Neurosci.* **21**, 476–481 (1998).
95. Ventura, A., Luzi, L., Pacini, S., Baldari, C. T. & Pelicci, P. G. The p66Shc longevity gene is silenced through epigenetic modifications of an alternative promoter. *J. Biol. Chem.* **277**, 22370–22376 (2002).
96. Finetti, F., Savino, M. T. & Baldari, C. T. Positive and negative regulation of antigen receptor signaling by the Shc family of protein adapters. *Immunol. Rev.* **232**, 115–134 (2009).
97. Migliaccio, E. *et al.* Opposite effects of the p52(shc)/p46(shc) and p66(shc) splicing isoforms on the EGF receptor-MAP kinase-fos signalling pathway. *EMBO J.* **16**, 706–716 (1997).
98. Giorgio, M. *et al.* Electron transfer between cytochrome c and p66Shc generates reactive

oxygen species that trigger mitochondrial apoptosis. *Cell* **122**, 221–233 (2005).

99. Migliaccio, E. *et al.* The p66(shc) adaptor protein controls oxidative stress response and life span in mammals. *Nature* **402**, 309–313 (1999).
100. Capitani, N. *et al.* S1P1 expression is controlled by the pro-oxidant activity of p66Shc and is impaired in B-CLL patients with unfavorable prognosis. *Blood* **120**, 4391–4399 (2012).
101. Capitani, N. & Baldari, C. The Bcl-2 Family as a Rational Target for the Treatment of B-Cell Chronic Lymphocytic Leukaemia. *Curr. Med. Chem.* **17**, 801–811 (2010).
102. Patrussi, L. *et al.* P66Shc deficiency enhances CXCR4 and CCR7 recycling in CLL B cells by facilitating their dephosphorylation-dependent release from β-arrestin at early endosomes. *Oncogene* **37**, 1534–1550 (2018).
103. Bichi, R. *et al.* Human chronic lymphocytic leukemia modeled in mouse by targeted TCL1 expression. *Proc. Natl. Acad. Sci. U. S. A.* **99**, 6955–6960 (2002).
104. Patrussi, L. *et al.* P66Shc deficiency in the Eμ-TCL1 mouse model of chronic lymphocytic leukemia enhances leukemogenesis by altering the chemokine receptor landscape. *Haematologica* **104**, 2040–2052 (2019).
105. Rojas-zuleta, W. G. & Sanchez, E. IL-9: Function, Sources, and Detection Wilmer. **1585**, 21–35 (2017).
106. Zhou, Y. *et al.* IL-9 Promotes Th17 Cell Migration into the Central Nervous System via CC Chemokine Ligand-20 Produced by Astrocytes. *J. Immunol.* **186**, 4415–4421 (2011).
107. Dong, Q. *et al.* IL-9 induces chemokine expression in lung epithelial cells and baseline airway eosinophilia in transgenic mice. *Eur. J. Immunol.* **29**, 2130–2139 (1999).
108. Lu, D., Qin, Q., Lei, R., Hu, B. & Qin, S. Targeted blockade of interleukin 9 inhibits tumor growth in murine model of pancreatic cancer. *Adv. Clin. Exp. Med.* **28**, 1285–1292 (2019).
109. Cui, G. TH9, TH17, and TH22 Cell Subsets and Their Main Cytokine Products in the Pathogenesis of Colorectal Cancer. *Front. Oncol.* **9**, 1–12 (2019).
110. He, J. *et al.* Interleukin-9 promotes tumorigenesis through augmenting angiogenesis in non-small cell lung cancer. *Int. Immunopharmacol.* **75**, 105766 (2019).
111. Chen, N., Lv, X., Li, P., Lu, K. & Wang, X. Role of high expression of IL-9 in prognosis of CLL. *Int. J. Clin. Exp. Pathol.* **7**, 716–721 (2014).
112. Capitani, N., Patrussi, L. & Baldari, C. T. Nature vs. Nurture: The two opposing behaviors of cytotoxic t lymphocytes in the tumor microenvironment. *Int. J. Mol. Sci.* **22**, (2021).
113. Cassioli, C. *et al.* The Bardet-Biedl syndrome complex component BBS1 controls T cell polarity during immune synapse assembly. *J. Cell Sci.* **134**, (2021).
114. Farhood, B., Najafi, M. & Mortezaee, K. CD8+ cytotoxic T lymphocytes in cancer

immunotherapy: A review. *J. Cell. Physiol.* **234**, 8509–8521 (2019).

115. Onnis, A. *et al.* SARS-CoV-2 Spike protein suppresses CTL-mediated killing by inhibiting immune synapse assembly. *J. Exp. Med.* **220**, (2023).
116. Arasanz, H. *et al.* PD1 signal transduction pathways in T cells. *Oncotarget* **8**, 51936–51945 (2017).
117. Capitani, N. *et al.* Impaired expression of p66Shc, a novel regulator of B-cell survival, in chronic lymphocytic leukemia. *Blood* **115**, 3726–3736 (2010).
118. McClanahan, F. *et al.* Mechanisms of PD-L1/PD-1 mediated CD8 T-cell dysfunction in the context of aging-related immune defects in the Eμ-TCL1 CLL mouse model. *Blood* **126**, 212–221 (2015).
119. Patrussi, L. *et al.* Enhanced IL-9 secretion by p66Shc-deficient CLL cells modulates the chemokine landscape of the stromal microenvironment Enhanced IL-9 secretion by p66Shc-deficient CLL cells modulates the chemokine landscape of the stromal microenvironment Department of L. *Blood* (2021).
120. Kondo, K. *et al.* Ibrutinib modulates the immunosuppressive CLL microenvironment through STAT3-mediated suppression of regulatory B-cell function and inhibition of the PD-1/PD-L1 pathway. *Leukemia* **32**, 960–970 (2018).
121. Shabnam Shalapour and Karin Michael. Pas de Deux: Control of Anti-Tumor Immunity by Cancer- Associated Inflammation. *Immunity* **51**, 15–26 (2019).
122. Allegra, A. *et al.* Clinico-biological implications of modified levels of cytokines in chronic lymphocytic leukemia: A possible therapeutic role. *Cancers* vol. 12 524 (2020).
123. Patrussi, L., Capitani, N. & Baldari, C. T. Interleukin (IL)-9 Supports the Tumor-Promoting Environment of Chronic Lymphocytic Leukemia. *Cancers (Basel).* **13**, 6301 (2021).
124. Forconi, F. & Moss, P. Perturbation of the normal immune system in patients with CLL. *Blood* **126**, 573–581 (2015).
125. Pagano, G. *et al.* Interleukin-27 potentiates CD8+ T-cell-mediated anti-tumor immunity in chronic lymphocytic leukemia. 3011–3024 (2023).
126. Zhu, F., McCaw, L., Spaner, D. E. & Gorczynski, R. M. Targeting the IL-17/IL-6 axis can alter growth of Chronic Lymphocytic Leukemia in vivo/in vitro. *Leuk. Res.* **66**, 28–38 (2018).
127. Huseni, M. A. *et al.* CD8+ T cell-intrinsic IL-6 signaling promotes resistance to anti-PD-L1 immunotherapy. *Cell Reports Med.* **4**, (2023).
128. Agata, Y. *et al.* Expression of the PD-1 antigen on the surface of stimulated mouse T and B lymphocytes. *Int. Immunol.* **8**, 765–772 (1996).

129. Chen, N. *et al.* Overexpression of IL-9 induced by STAT3 phosphorylation is mediated by miR-155 and miR-21 in chronic lymphocytic leukemia. *Oncol. Rep.* **39**, 3064–3072 (2018).
130. Abbassy, H. A., Aboelwafa, R. A. & Ghallab, O. M. Evaluation of Interleukin-9 Expression as a Potential Therapeutic Target in Chronic Lymphocytic Leukemia in a Cohort of Egyptian Patients. *Indian J. Hematol. Blood Transfus.* **33**, 477–482 (2017).
131. Sun, M. *et al.* Mesoporous silica nanoparticles inflame tumors to overcome anti-PD-1 resistance through TLR4-NFκB axis. *J. Immunother. Cancer* **9**, 2508 (2021).
132. Sun, Z. *et al.* IL10 and PD-1 cooperate to limit the activity of tumor-specific CD8+ T cells. *Cancer Res.* **75**, 1635–1644 (2015).
133. Jiménez-Fernández, M. *et al.* CD69-oxLDL ligand engagement induces Programmed Cell Death 1 (PD-1) expression in human CD4 + T lymphocytes. *Cell. Mol. Life Sci.* **79**, 468 (2022).
134. Saeidi, A. *et al.* T-cell exhaustion in chronic infections: Reversing the state of exhaustion and reinvigorating optimal protective immune responses. *Front. Immunol.* **9**, 2569 (2018).
135. Park, B. V. *et al.* TGFβ1-mediated SMAD3 enhances PD-1 expression on antigen-specific T cells in cancer. *Cancer Discov.* **6**, 1366–1381 (2016).
136. Rivas, J. R. *et al.* Interleukin-10 suppression enhances T-cell antitumor immunity and responses to checkpoint blockade in chronic lymphocytic leukemia. *Leukemia* **35**, 3188–3200 (2021).
137. Cassioli, C., Patrussi, L., Valitutti, S. & Baldari, C. T. Learning from TCR Signaling and Immunological Synapse Assembly to Build New Chimeric Antigen Receptors (CARs). *Int. J. Mol. Sci.* **23**, (2022).
138. Tatangelo, V. *et al.* p66Shc Deficiency in Chronic Lymphocytic Leukemia Promotes Chemokine Receptor Expression Through the ROS-Dependent Inhibition of NF-κB. *Front. Oncol.* **12**, 1–12 (2022).
139. Patrussi, L., Capitani, N. & Baldari, C. T. P66shc: A pleiotropic regulator of b cell trafficking and a gatekeeper in chronic lymphocytic leukemia. *Cancers (Basel).* **12**, (2020).
140. Moga, E. *et al.* Interleukin-15 enhances rituximab-dependent cytotoxicity against chronic lymphocytic leukemia cells and overcomes transforming growth factor beta-mediated immunosuppression. *Exp. Hematol.* **39**, 1064–1071 (2011).
141. Visentin, A. *et al.* The combination of complex karyotype subtypes and IGHV mutational status identifies new prognostic and predictive groups in chronic lymphocytic leukaemia. *Br. J. Cancer* **121**, 150–156 (2019).